Published for SISSA by Springer

Received: October 27, 2022
Revised: December 7, 2022
Accepted: December 14, 2022
Published: January 4, 2023

Relic challenges for vector-like fermions as connectors to a dark sector

Alexandre Carvunis,[a,b,c] **Navin McGinnis**[c] **and David E. Morrissey**[c]

[a] *École normale supérieure Paris-Saclay, 4 Av. des Sciences, 91190 Gif-sur-Yvette, France*
[b] *Laboratoire d'Annecy-le-Vieux de Physique Théorique, Université de Savoie Mont-Blanc et CNRS, B.P. 110, F-74941, Annecy Cedex, France*
[c] *TRIUMF, 4004 Wesbrook Mall, Vancouver, BC, V6T 2A3, Canada*

E-mail: a.carvunis@ip2i.in2p3.fr, nmcginnis@triumf.ca, dmorri@triumf.ca

Abstract: New dark sectors consisting of exotic fields that couple only very feebly to the Standard Model (SM) have strong theoretical motivation and may be relevant to explaining the abundance of dark matter (DM). An important question for such sectors is how they connect to the SM. For a dark sector with a new gauge interaction, a natural connection arises from heavy vector-like fermions charged under both the visible and dark gauge groups. The gauge charges of such fermions imply that one or more of them is stable in the absence of additional sources of dark symmetry breaking. A generic challenge for such connectors is that they can produce too much dark matter or interact too strongly with nuclei if they were ever thermalized in the early universe. In this paper we study this challenge in a simple connector theory consisting of new vector-like electroweak doublet and singlet fermions that also transform under the fundamental representation of a new Abelian gauge force, and we show that these connectors in their minimal form are almost always ruled out by existing direct DM searches. To address this challenge, we investigate two solutions. First, we study mitigating scattering on nuclei by introducing a Majorana mass term for the singlet. And second, we investigate a mixing with SM leptons that allows the connectors to decay while remaining consistent with cosmological tests and searches for charged lepton flavour violation. Both solutions rely on the presence of a dark Higgs field with a specific charge.

Keywords: Models for Dark Matter, Vector-Like Fermions, Cosmology of Theories BSM, Dark Matter at Colliders

ArXiv ePrint: 2209.14305

https://doi.org/10.1007/JHEP01(2023)014

JHEP01(2023)014

Contents

JHEP01(2023)014

1 Introduction

New gauge forces arise in many well-motivated extensions of the Standard Model (SM) [1–4]. These forces are said to be dark if they do not couple directly to the matter of the SM. Dark forces may also connect to dark matter (DM) and play a crucial role in determining its properties and abundance today [5–9].

Despite their name, dark forces are usually the most interesting when they are not completely dark and interact with the SM [10, 11]. The most thoroughly studied realization of a dark force involves a new $\mathrm{U}(1)_x$ Abelian gauge group with a massive *dark photon* that couples to the SM through kinetic mixing with hypercharge [12, 13],

$$-\mathscr{L} \supset \frac{\epsilon}{2\,c_W} B_{\mu\nu} X^{\mu\nu}\,, \tag{1.1}$$

where $X_{\mu\nu} = (\partial_\mu X_\nu - \partial_\nu X_\mu)$ is the field strength of the new vector field X_μ and ϵ is the dimensionless kinetic mixing parameter. This operator is one of three renormalizable portals through which a new SM singlet can connect to the SM. The phenomenological and cosmological implications of dark photons have been studied extensively over an enormous range of masses and kinetic mixings [14, 15]. In particular, there is broad ongoing program of accelerator-based searches for visibly or invisibly decaying dark photons with expected (but incomplete) sensitivity for $m_\chi \sim 10$ MeV–100 GeV and $\epsilon \gtrsim 10^{-6}$ [10, 11, 14–18].

While the experimental and astrophysical implications of dark phtons have been studied in detail, less attention has been paid to the physics giving rise to the kinetic mixing operator of eq. (1.1). The canonical origin for kinetic mixing in the range $\epsilon \sim 10^{-8}$–10^{-2} is connector matter charged under both hypercharge and the dark gauge group [8, 13, 19, 20]. If such matter breaks the dark-sector charge conjugation symmetry present in the limit $\epsilon \to 0$, it generates a non-zero kinetic mixing through loops. In the absence of further structure in the theory, we can make two definite statements about such connectors based on dark gauge invariance. First, being charged under Abelian groups, they must come in the form of complex scalars or Dirac fermions (for spins $s < 1$; higher spins come with additional complications). And second, the lightest connector state is stable.

We argue that these general requirements for connector matter have important observational implications if the early universe was ever hot enough to produce them with a thermal abundance. Being stable, the lightest connector state will contribute to the total density of dark matter (DM). Assuming a standard cosmology after inflationary reheating, this requires that the lightest connector be below several tens of TeV in mass to avoid overclosing the universe [21], and closer to the TeV scale if the relevant annihilation channels are perturbatively weak [22]. This implies three distinct possibilities for viable dark sector connectors: i) they must be heavy enough to have avoided significant cosmological production after inflationary reheating or a later dilutionary event; ii) or they must be light enough that they are potentially observable; iii) or some additional structure is needed in the dark sector. We focus on the second and third possibilities in this work.[1]

Stable relic connectors must satisfy additional requirements to be consistent with observations. Relics charged under electromagnetism [23] or the strong force [24] tend to be problematic and this drives us to consider connector quantum numbers that yield an electrically neutral, colour-singlet lightest state. Since the connectors carry hypercharge by assumption, at least some of them must also be charged under $\mathrm{SU}(2)_L$ to yield a neutral state with $t_L^3 = -Y$, and this implies that the neutral state also couples to the Z boson. Moreover, since the relics transform under complex representations they develop very large scattering cross sections on nuclei from the vectorial exchange of Z of X bosons [25, 26]. Such cross sections are typically strongly ruled out by direct detection searches for dark matter (DM) [27], even if the stable relic makes up only a tiny fraction of the total DM abundance. This presents a generic challenge for connector matter; the goal of our work is to illustrate this challenge and examine the additional structure needed in the dark sector to overcome it.

[1] Hypercharged connectors contribute to the Higgs mass parameter at two-loop order and thus electroweak naturalness may disfavor possibility i).

JHEP01(2023)014

Let us also point out that theories with both a dark photon and connector matter near the weak scale have broad phenomenological motivation and have been proposed to address various anomalies. For one, the lightest connector state itself can be a viable candidate for DM in some cases. Other applications include dark photon connectors considered in relation to the muon magnetic moment anomaly in ref. [28], as an explanation for B-physics and cosmic ray anomalies in ref. [29], and as an enabling mechanism for exotic Higgs decays in refs. [28, 30]. Dark- and SM-charged fermions arise in many proposals to address the electroweak hierarchy problem [31–34]. Such multiplets may also be expected in unification scenarios where the SM and $\mathrm{U}(1)_x$ gauge groups are descendants of a single gauge group [35, 36]. We note further related studies of connector matter in refs. [37–43].

To illustrate the general relic and direct detection challenges to dark sector connectors, and to provide a base on which to extend the dark sector itself, we focus on a specific realization of connector matter. Specifically, we consider two exotic vector-like fermion multiplets with charge assignments under $\mathrm{SU}(3)_c \times \mathrm{SU}(2)_L \times \mathrm{U}(1)_Y \times \mathrm{U}(1)_x$ of $N = (1, 1, 0; q_x)$ and $P = (1, 2, -1/2; q_x)$. This allows the Higgs Yukawa coupling and mass terms

$$-\mathscr{L} \supset \left(\lambda \overline{P} \widetilde{H} N + \text{h.c.}\right) + m_P \overline{P} P + m_N \overline{N} N \,, \tag{1.2}$$

where $\widetilde{H} = i\sigma_2 H^*$. The new parameters m_P, m_N, and λ can all be taken to be real and positive through field redefinitions. We also normalize the dark gauge coupling g_x such that $q_x = 1$. Coupling the connectors to the SM Higgs breaks what would otherwise be independent flavor symmetries in each multiplet that would produce two stable states. Our specific choice of connectors is motivated by obtaining a single potentially viable neutral relic particle, in contrast to electromagnetically or strongly charged relics. This choice can be generalized to larger representations of $\mathrm{SU}(2)_L$ with appropriate hypercharges [44]. For $m_P \ll m_N$, this model approaches the limit of a pure $\mathrm{SU}(2)_L$ multiplet connector, while for $m_N \ll m_P$ it approximates minimal secluded dark matter [7].

After electroweak symmetry breaking, the new fermions mix to form a pair of neutral Dirac fermions ψ_1 and ψ_2 as well as a charged Dirac fermion P^-. The ψ_1 is the lightest connector state and is stable in this minimal theory. For moderate to small λ and $\alpha_x = g_x^2/4\pi$ we find that it must be lighter than a few TeV to avoid producing too much dark matter. As expected on general grounds, it has very large nucleon scattering cross sections through X or Z exchange. We show that is nearly always ruled out by direct detection experiments, even when the ψ_1 relic density makes up only a small fraction of the total dark matter abundance.

To address this challenge we investigate two extensions of the minimal connector fermion model, discussed previously in refs. [28, 30] but not studied there in detail. In the first extension, we introduce an explicit dark Higgs field Φ with $q_\Phi = -2q_x$ that develops a vacuum expectation value and can induce a Majorana mass for the fermions. This splits the neutral Dirac fermion states into pseudo-Dirac pairs with only off-diagonal couplings to the vector bosons and eliminates the leading contributions to nucleon scattering. We show that this can be sufficient for consistency with current direct dark matter searches and that ψ_1 can even be the source of dark matter. The second extension uses a dark Higgs field ϕ with $q_\phi = q_x$ to mix the connector doublet with the lepton doublets of the SM. This coupling

JHEP01(2023)014

allows all the connector fermions to decay to SM states, but can also lead to charged lepton flavour violation (LFV). We demonstrate that there exits a range of small couplings that are allowed by current LFV limits and that also permit all the connector fermions to decay early enough to avoid bounds from energy injection in the early universe [45, 46].

A common feature of both of these extensions of the minimal connector theory is the presence of an explicit dark Higgs field with a dark charge that allows it to couple to at least some of the connectors. In the context of the general arguments about connector matter presented above, we see that the dark Higgs is needed to absorb the dark charge of the lightest connector to allow it to obtain a Majorana mass or decay to SM states (that do not carry dark charge by definition). This appears to be a general requirement that goes beyond the specific connector example we have studied. The natural mass for such a dark Higgs is similar to or less than the dark photon, barring a very small gauge coupling, and this motivates direct searches for the scalar field it gives rise to [47–52]. In contrast, for a dark photon whose mass comes from the Stueckelberg mechanism our results suggest that the origin of kinetic mixing should be relatively heavy.

The outline of this paper is as follows. After this introduction we present in section 2 our benchmark minimal singlet-doublet theory of connector fermions and we study the laboratory bounds on the new states that it predicts. Next, in section 3 we investigate the thermal freezeout and dark matter signals of the stable ψ_1 fermion. In section 4 we present a simple extension of the theory with a Majorana mass term that helps to alleviate the strong bounds we find on the minimal theory from direct detection. In section 5 we study a second extension of the minimal model that allows all the connector fermions to ultimately decay down to the SM through lepton mixing and investigate the resulting implications. Finally, section 6 is reserved for our conclusions. Some additional results are listed in an appendix A.

2 Review of the minimal theory and laboratory bounds

We begin by studying the masses, interactions, and direct laboratory bounds on the minimal fermionic connector theory consisting of vector-like fermions $P = (1, 2, -1/2; q_x)$ and $N = (1, 1, 0; q_x)$ charged under a new $\mathrm{U}(1)_x$ gauge invariance with massive boson X^μ. Our primary focus is on lighter dark vector bosons with $m_x \ll m_Z$. We also normalize the dark gauge coupling such that $q_x = 1$ without loss of generality.

2.1 Masses and interactions

Electroweak symmetry breaking leads to mass mixing between the neutral components of the P and N fermions. Taking $H \to (0, v + h/\sqrt{2})$ in unitary gauge, the resulting spectrum of connector fermions consists of a charged fermion P^- with mass m_P from the doublet together with two neutral Dirac fermions ψ_1 and ψ_2 with masses

$$m_{1,2} = \frac{1}{2}\left[m_N + m_P \mp \sqrt{(m_N - m_P)^2 + 4\lambda^2 v^2}\right], \tag{2.1}$$

JHEP01(2023)014

and mixing angles

$$\begin{pmatrix} N \\ P^0 \end{pmatrix} = \begin{pmatrix} c_\alpha & s_\alpha \\ -s_\alpha & c_\alpha \end{pmatrix} \begin{pmatrix} \psi_1 \\ \psi_2 \end{pmatrix} , \tag{2.2}$$

where

$$\tan(2\alpha) = \frac{2\lambda v}{m_P - m_N} . \tag{2.3}$$

We choose the solution for α such that $m_1 < m_2$. The couplings of these states to the SM Higgs and electroweak vector bosons are collected in ref. [30]. Given the very strong direct bounds on light, electroweakly-charged fermions [53], we only consider parameters such that $m_1 > 0$ corresponding to the condition $\sqrt{m_N m_P} > \lambda\, v$.

Our theory also contains a new $\mathrm{U}(1)_x$ vector boson X^μ with gauge coupling $g_x \equiv \sqrt{4\pi\,\alpha_x}$. We assume that this vector obtains a mass m_x from either a dark Higgs [7, 8] or Stueckelburg mechanism [54, 55]. In addition to its direct gauge interactions with the new fermions (all with dark charge $q_x = 1$ here), the new vector connects with the SM through gauge kinetic mixing with hypercharge [12, 13],

$$-\mathscr{L} \supset \frac{\epsilon}{2\,c_W} B_{\mu\nu} X^{\mu\nu} . \tag{2.4}$$

The mixing parameter ϵ allows the dark vetor to decay and receives direct contributions from loops of the new P fermions. For $m_1 \gg m_x$, which is the scenario we focus on here, the mediator fermions contribute an inhomogeneous term to the renormalization group running of ϵ from a given ultraviolet scale μ down to m_P of

$$\begin{aligned} \Delta\epsilon &\simeq -\frac{1}{3\pi}\sqrt{\alpha\,\alpha_x}\,\ln\left(\frac{\mu}{m_P}\right) \\ &\simeq -(3\times 10^{-3})\left(\frac{\alpha_x}{10\,\alpha}\right)^{1/2}\ln\left(\frac{\mu}{m_P}\right) . \end{aligned}$$

This suggests a natural size of the kinetic mixing on the order of $|\epsilon| \sim 10^{-3}$. Let us note, however, that the mixing can be eliminated or made parametrically small without fine tuning by introducing a mirror copy of the connector fermions with opposite $\mathrm{U}(1)_x$ charges and a small breaking of the mass degeneracy between them [20, 56, 57]. As a concrete benchmark for the dark vector in this work, we focus on $m_x \simeq 15$ GeV and $|\epsilon| \sim 10^{-4}$–10^{-3} corresponding to a natural one-loop range.

The massive fermions also generate an effective coupling of the SM Higgs boson to dark vectors at one-loop order. In the limit of $m_h \ll m_{1,2}$, the leading term is [30, 58]

$$\mathscr{L} \supset \frac{\alpha_x}{6\pi}\frac{\lambda^2}{m_1 m_2} H^\dagger H\, X_{\mu\nu} X^{\mu\nu} . \tag{2.5}$$

A full expression for the loop function producing this operator is given in ref. [30].

2.2 Laboratory bounds on the theory

The new particles in the theory are constrained by direct tests of the dark vector boson, precision electroweak measurements, collider searches at LEP and the LHC, and exotic

JHEP01(2023)014

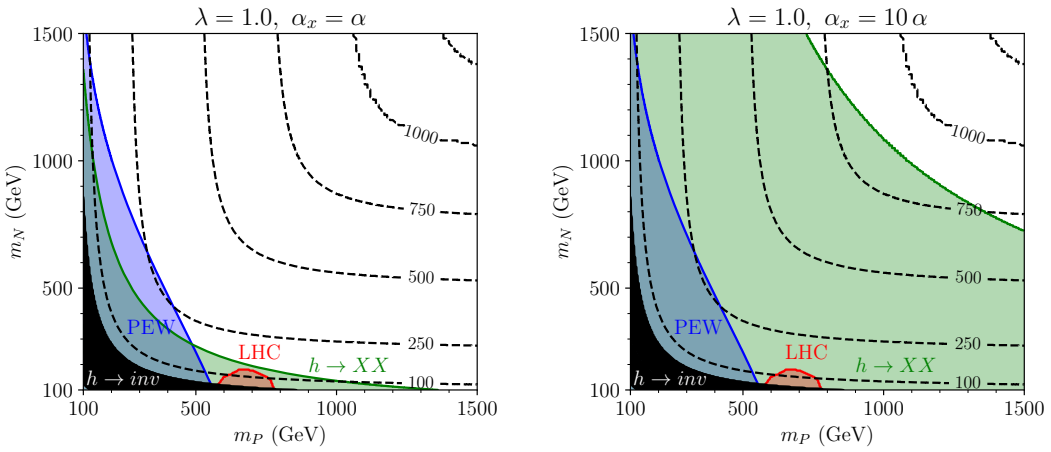

Figure 1. Laboratory bounds on the connector fermions in the m_P–m_N plane for $\lambda = 1.0$, and $\alpha_x = \alpha$ (left) and $\alpha_x = 10\alpha$ (right). The solid black region is excluded by invisible Higgs boson decays ($h \to inv$), the shaded green region indicates bounds from $h \to XX$ decays, the blue region shows exclusions from precision electroweak tests (PEW), and the red region denotes bounds from direct searches at the LHC. The dashed lines are contours of constant ψ_1 masses m_1 in GeV.

Higgs decays. We investigate the most important of these direct constraints here, updating and expanding the earlier analysis of ref. [30]. Our results are summarized in figure 1, which shows the exclusions we find in the m_P–m_N plane for $\lambda = 1.0$, together with $\alpha_x = \alpha$ (left) and $\alpha_x = 10\,\alpha$ (right). The dashed lines in this figure indicate contours of constant ψ_1 mass m_1.

For our benchmark dark vector mass of $m_x = 15$ GeV, the strongest current direct bound on the dark vector [15] comes from the LHCb search for $X^\mu \to \mu^+\mu^-$ of ref. [59], implying $|\epsilon| \lesssim 10^{-3}$ in this mass region. Searches for dimuon resonances at CMS also provide a similar constraint [60]. These limits are consistent with the range of kinetic mixings we consider.

Mixing between the singlet and doublet can modify electroweak observables. The deviations induced are captured well by the oblique parameters S, T, and U [61, 62]. Full expressions for the shifts in these parameters are given in ref. [30]. We apply these results to compute S, T, and U in the theory and compare them to the experimentally obtained values and correlations collected in ref. [63] to derive exclusions.[2] These exclusions are shown in figure 1 for $\lambda = 1.0$.

The coupling of the P and N fermions to the Higgs field can give rise to non-standard Higgs boson decay channels. If $m_1 < m_h/2$, the invisible decay $h \to \psi_1\bar{\psi}_1$ proceeds with partial width

$$\Gamma(h \to \psi_1\bar{\psi}_1) = \frac{\lambda^2 \sin^2(2\alpha)}{16\pi}\, m_h \left[1 - \left(\frac{2m_1}{m_h}\right)^2\right]^{3/2} . \tag{2.6}$$

[2] We use the Particle Data Group [63] combined value of the W mass in our evaluation that does not include the recent, larger value obtained by the CDF collaboration [64].

JHEP01(2023)014

Comparing to the SM Higgs width of $\Gamma_h \simeq 4.1$ MeV, the branching fraction of this channel easily exceeds the recent ATLAS limit on invisible Higgs decays of $\mathrm{BR}(h \to inv) < 0.145$ [65] over essentially the entire parameter space we consider (with $\lambda \geq 0.1$). The corresponding exclusions are shown in figure 1.

More visibly, loops of the heavy fermions give rise to $h \to XX$ decays which can produce highly distinctive pairs of dilepton resonances. For $m_{1,2} \gg m_h$, this is described well by the effective operator of eq. (2.5) yielding the partial width

$$\Gamma(h \to XX) = \frac{\alpha_x^2}{72\pi^3}\left(\frac{\lambda^2 v^2}{m_1 m_2}\right)^2 \frac{m_h^3}{v^2}\left[1 - \left(\frac{2m_x}{m_h}\right)^2 + 6\left(\frac{m_x}{m_h}\right)^4\right]\sqrt{1-\left(\frac{2m_x}{m_h}\right)^2}. \tag{2.7}$$

This decay channel has been searched for by ATLAS [66] and CMS [67], with the former analysis giving the most stringent bound for $m_x = 15$ GeV of $\mathrm{BR}(h \to XX) < 2.35 \times 10^{-5}$. The decay can also be mediated directly by kinetic mixing [68], but the associated branching ratio scales like ϵ^4 and is strongly subleading relative to the loop decay for the parameters considered here. Bounds from $h \to XX$ are given in figure 1, and are particularly strong for larger λ and α_x, but fall off quickly for smaller λ or α_x (scaling like $\alpha_x^2\lambda^4$). Loops as well as kinetic mixing also give rise to $h \to XZ$, but we find that the resulting constraints are not as strong as those from $h \to XX$.

Collider searches are sensitive to the heavier connector fermions to the extent that they can be created efficiently. In the minimal doublet-singlet P–N model considered in this work, the production and decay channels are analogous to a Higgsino-Bino system in the minimal supersymmetric Standard Model [69] and the associated collider signals are very similar [70–72]. Based on this analogy, collider bounds on the theory from LEP and the LHC were estimated in ref. [30]. Results from LEP constrain $m_P \gtrsim 90$–100 GeV depending on the mass splitting between the $P^\pm$ and ψ_1 states. Here, we focus on m_P, $m_N \geq 100$ GeV and derive updated limits from new LHC data.

Pair production of the connector fermions at the LHC occurs predominantly through s-channel Drell-Yan processes with γ/Z or W boson exchanges. The rates for these processes therefore depend on the doublet content of the relevant states. Once created, the connector fermions decay down to the lightest state ψ_1 through $P^\mp \to W^{\mp\,(*)}\psi_1$ or $\psi_2 \to h/Z^{(*)}\psi_1$. These considerations imply that up to mixing effects, the fermions are the most detectable for the mass hierarchy $m_N < m_P$. The $P^\mp$ and ψ_2 states are then analogous to the $\chi_1^\mp$ and $\chi_{2,3}^0$ states of a Higgsino-Bino system for $|M_1| < |\mu|$, with LHC signatures involving significant missing energy and the decay products of the electroweak bosons. When $m_P < m_N$, the mostly-doublet states tend to be close in mass and their decay products are soft and difficult to detect.

Recently the ATLAS collaboration has performed a comprehensive search for the chargino-neutralino system that targets Higgsino-Bino signals [73]. To estimate the bounds on connector fermions implied by this search we calculate production cross sections using `MadGraph5` [74] where the couplings and mass eigenstates were implemented using `FeynRules 2.3` [75]. We consider all possible decay chains of $P^\pm$ and ψ_2 into EW and Higgs bosons and estimate the corresponding strength of each signal in the signal regions identified as 4Q-VV, 2B2Q-WZ, and 2B2Q-Wh in the analysis of ref. [73] using the datasets of

JHEP01(2023)014

efficiencies and detector acceptances available from the HEPData page of the corresponding search [73]. Using the provided SM backgrounds for each region, the combined significance is then calculated for a given λ, m_P, and m_N using the asymptotic approximations given in [76]. We show the resulting 95% CL exclusion regions in the m_P-m_N plane for $\lambda = 1.0$ in figure 1. Our results align closely with those presented in [73] for the Higgsino-Bino system as expected.

The collected model bounds shown in figure 1 correspond to the relatively large value $\lambda = 1.0$. As λ decreases, many of these bounds weaken significantly. For $\lambda = 0.1$, we find that the only remaining direct bound in the parameter space shown comes from LHC searches and is nearly identical to the $\lambda = 1.0$ case. Let us also point out that large values of λ tend to destabilize the Higgs potential by driving the Higgs quartic coupling negative at a lower scale than in the SM. This effect was studied in ref. [30], and for the parameters considered in this work the scenario can be treated as a self-consistent effective theory up to energies of at least 5 TeV.

3 Dark matter in the minimal connector theory

The analysis in the previous section shows that the new connector fermions are safe from direct collider searches and precision electroweak tests for masses $m_1 \gtrsim 100$–700, GeV, depending on the specific mass spectrum and coupling strengths. Even stronger bounds can be derived on the theory from the contribution of the lightest stable new fermion ψ_1 to the abundance of dark matter and signals in direct dark matter searches. In particular, the vector couplings of ψ_1 lead to direct detection rates that are nearly always ruled out, even when this state only makes up a small fraction of the total dark matter density.

3.1 Relic densities

Thermal reactions in the early universe would have created the exotic fermions ψ_1, ψ_2, and $P^{\mp}$ with significant abundances if the temperature was ever hot enough, $T \gtrsim m_1/20$. The fermions would have then undergone thermal freezeout as the universe cooled to produce a relic density of neutral ψ_1 particles. We assume that this occured with no subsequent large injections of entropy to dilute their relic density beyond the standard expansion of spacetime.

To compute the ψ_1 relic abundance, we have implemented the theory in `FeynRules 2.3` [75, 77, 78] and interfaced it with `MadDM v3.2` [79–81]. We show the resulting ψ_1 relic densities ρ_1 relative to the observed dark matter abundance $\rho_{\rm DM}$ in figure 2 as a function of the mass parameters m_P and m_N for $\lambda = 0.1$ (top) and $\lambda = 1.0$ (bottom), together with $\alpha_x = \alpha$ (left) and $\alpha_x = 10\alpha$ (right). For these coupling values, we expect that non-perturbative enhancements of the annihilation cross section at freeze-out will be negligible to mild [8, 82, 83]. The grey shaded regions in these plots summarize the exclusions from direct laboratory searches as discussed in section 2.2. In the black shaded regions the ψ_1 thermal relic density exceeds the observed value and is therefore ruled out. Along the boundary of this region, shown by a white dashed line, the ψ_1 relic makes up all the dark matter.

JHEP01(2023)014

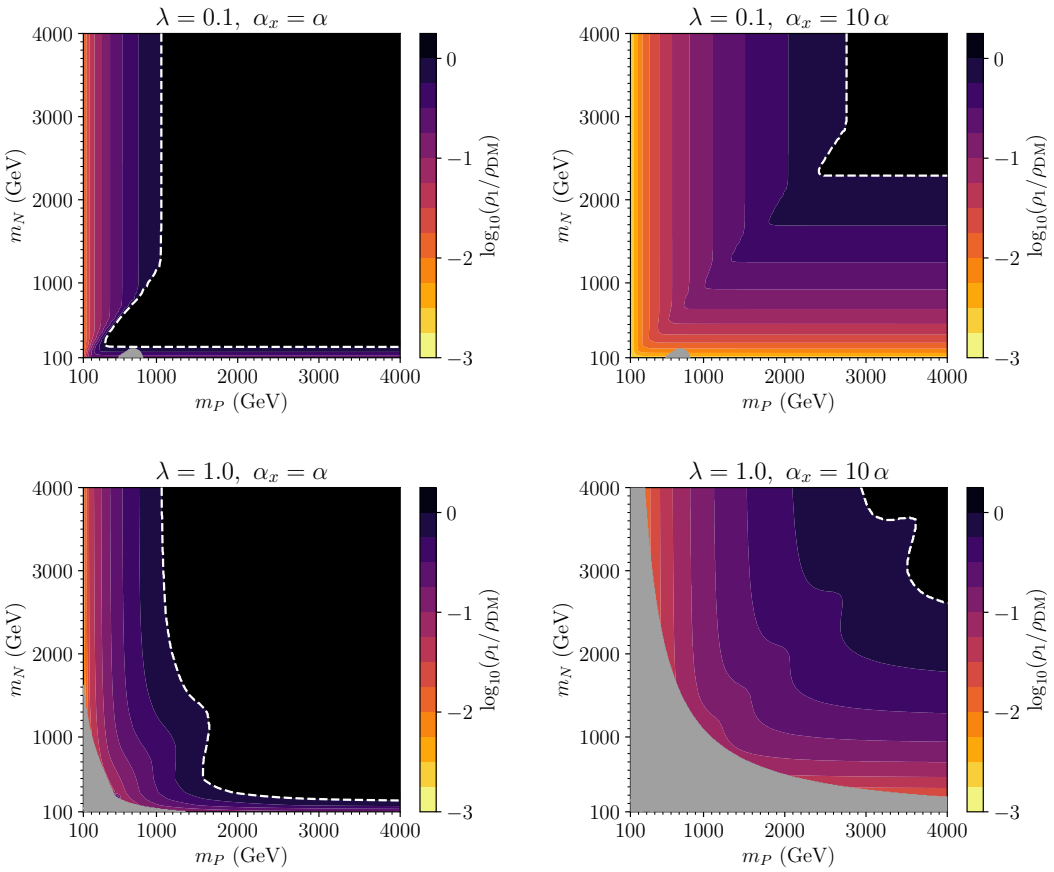

Figure 2. Fractional relic densities $\rho_1/\rho_{\rm DM}$ of the ψ_1 connector fermion for $\lambda = 0.1$ (top) and $\lambda = 1.0$ (bottom) with $\alpha_x = \alpha$ (left) and $\alpha_x = 10\,\alpha$ (right). The grey shaded regions show the combined exclusions from direct searches while the black shaded regions indicate where ψ_1 produces too much thermal dark matter.

Since we focus on the limit $m_1 \gg m_x$, while direct bounds typically require $m_1 \gtrsim m_Z$, the ψ_1 state always has efficient annihilations to at least some vector bosons in the parameter regions of interest, $\psi_1 + \bar{\psi}_1 \to V + V$ where $V = X, Z, W$. When $m_P < m_N$ and $m_P \gg \lambda\, v$, the ψ_1 and P^- masses tend to be close to each other and coannihilation can be significant. These features are evident in figure 2. For larger $\alpha_x = 10\,\alpha$, DM annihilation is dominated by $\psi_1 + \bar{\psi}_1 \to X + X$ and the relic abundance depends mainly on m_1. In contrast, for smaller $\alpha_x = \alpha$ annihilations to weak vector bosons become important and we see a more efficient depletion of the relic density when ψ_1 is composed mainly of P^0 ($m_P < m_N$) relative to when it is mostly N^0 ($m_N < m_P$). Indeed, with $m_P \gg m_N$ the ψ_1 state is analogous to a pure Higgsino lightest superpartner in supersymmetry with $\mu \sim m_P \sim m_1$, and the correct relic density is obtained for the familiar value of $m_P \simeq 1100$ GeV [84–86].

The relic densities shown in figure 2 generally grow larger as the mass m_1 increases. Even for larger dark-sector couplings $\alpha_x = 10\,\alpha$, the ψ_1 relic produces too much dark matter if $m_1 \gtrsim 3$ TeV. This illustrates the general argument about connector relic densities made

JHEP01(2023)014

in the introduction, and provides a further motivation for at least some of them to not be too heavy beyond considerations of naturalness.

3.2 Constraints from direct detection

While the lightest connector fermion ψ_1 can have an acceptably small relic density, it is a Dirac fermion that interacts with nuclei with an unsuppressed spin-independent interaction mediated by the Z and X vector bosons. This can lead to very large cross sections on nuclei that are in tension with searches from direct detection experiments, even when the ψ_1 states makes up only a very small fraction of the total DM abundance [28, 30].

The leading spin-independent (SI) per-nucleon cross section on a target nucleus $N = (A, Z)$ is [25]

$$\sigma_{\rm SI} = \frac{\mu_n^2}{\pi}\left[\frac{Z f_p + (A-Z) f_n}{A}\right]^2 , \tag{3.1}$$

where $\mu_n = m_n m_1/(m_n + m_1)$ is the DM-nucleon reduced mass, and

$$f_p = \frac{G_F}{\sqrt{2}} s_\alpha^2 (1 - 4 s_W^2) - \frac{4\pi}{m_x^2}\epsilon\sqrt{\alpha\alpha_x} - \tilde{d}_p\left[\frac{2}{9} + \frac{7}{9}\sum_q f_q^p\right] , \tag{3.2}$$

$$f_n = -\frac{G_F}{\sqrt{2}} s_\alpha^2 + 0 - \tilde{d}_n\left[\frac{2}{9} + \frac{7}{9}\sum_q f_q^n\right] . \tag{3.3}$$

The three terms in each of these expressions correspond to Z, X, and Higgs exchange, respectively. For the Higgs terms, the sums run over light quarks $q = u, d, s$, the coefficients $f_q^{p,n}$ are collected in ref. [26], and the couplings $\tilde{d}_{p,n}$ are given by

$$\tilde{d}_p = \tilde{d}_n = -\frac{m_n}{2\,v}\frac{\lambda\,\sin(2\alpha)}{m_h^2} , \tag{3.4}$$

for the Higgs mass m_h.

Combining these cross sections with the relic densities above, we can estimate the experimental bounds on the connector fermions from direct detection experiments. For spin-independent scattering in the mass range of interest, $m_1 \gtrsim 100$ GeV, the most stringent current limits come from LUX-ZEPLIN [27]. For a given ψ_1 mass, we compare the stated limit on the per-nucleon cross section $\sigma_{\rm SI}$ to the density-weighted value $(\rho_1/\rho_{\rm DM})\,\sigma_{\rm SI}$ derived here assuming a xenon target.

In figure 3 we show contours of the density-weighted, spin-independent per nucleon cross section $\sigma_{\rm SI}\,\rho_1/\rho_{\rm DM}$ in the m_P–m_N plane for $\lambda = 0.1, 1.0$ (top and bottom) and $\alpha_x = \alpha,\ 10\,\alpha$ (left and right). We also fix the kinetic mixing at $\epsilon = -10^{-4}$ for reference. The downward hatched regions in these panels show the current exclusions from direct detection searches [27]. As before, the filled grey regions show the combined bounds from laboratory searches for the connector fermions while the black regions indicate where the thermal relic density of ψ_1 exceeds the observed value.

Nearly the entire parameter region consistent with laboratory searches and the ψ_1 relic density shown in the panels of figure 3 is ruled out by direct detection searches. This is despite the ψ_1 relic density often only making up a very small fraction of the total

JHEP01(2023)014

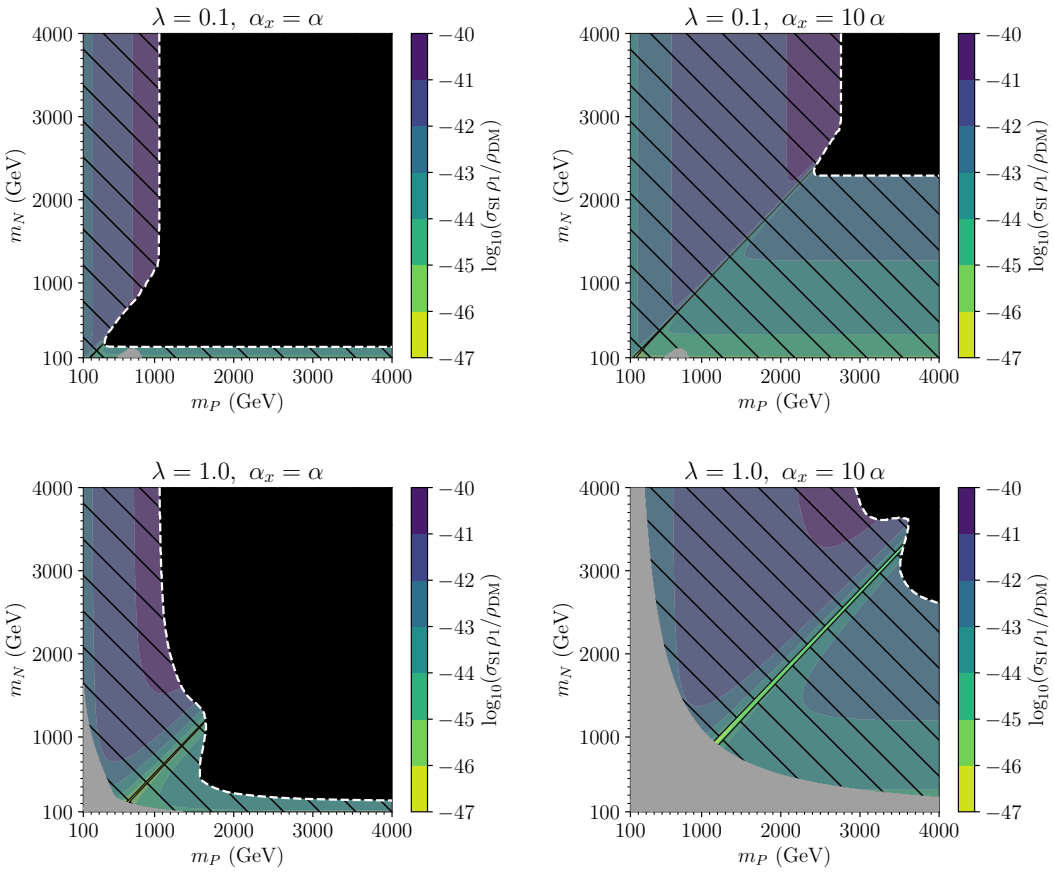

Figure 3. Contours of the density-weighted spin-independent per nucleon cross section ($\sigma_{\rm SI}\,\rho_1/\rho_{\rm DM}$) for the minimal connector theory in the m_P–m_N plane for $\lambda = 0.1, 1.0$ (top and bottom) and $\alpha_x = \alpha, 10\,\alpha$ (left and right). The downward hatched regions are excluded by DM direct detection searches, the grey shaded regions show the combined exclusions from direct searches, and the black regions indicate where ψ_1 produces too much thermal dark matter.

dark matter density. The strong exclusions come from the direct vector couplings of ψ_1 to nucleons through the Z^0 and X vector bosons, which avoid the suppression by small Yukawa couplings or loops seen in Higgs boson exchange. The only parameter region not excluded is a very thin sliver where the various contributions to the effective SI cross section cancel almost completely. This occurs for negative ϵ, which we have chosen here to illustrate the effect. We conclude from figure 3 that the minimal connector fermion scenario is all but ruled out assuming a standard, thermal cosmological history.

4 Moderated signals from a majorana mass term

Having found that the connector fermions in the theory are nearly completely excluded by direct dark matter searches, we turn now to ways to mitigate their impact on direct detection. As a first approach, we expand the minimal theory with an explict dark Higgs

JHEP01(2023)014

field Φ with $\mathrm{U}(1)_x$ charge $q_\Phi = -2q_x$. This allows the new Yukawa coupling

$$-\mathscr{L} \supset \frac{1}{2} y_N \, \Phi \, \overline{N^c} N + \text{h.c.} \tag{4.1}$$

where we have given equal masses to both Weyl components for simplicity. If Φ develops a VEV, $\langle \Phi \rangle = \eta$, the new coupling generates a Majorana mass term $M = y_N \eta$ for the SM-singlet N fermion. This separates the two Weyl components of the Dirac fermion ψ_1 into a pair of Majorana fermions with mass splitting Δm. For $\Delta m \ll m_1$ such a splitting implies primarily off-diagonal couplings to the Z and X vector bosons [87], which strongly suppresses nuclear scattering through vector exchange for $\Delta m \gtrsim 200\,\text{keV}$ [88, 89]. Instead, the dominant contribution to nuclear scattering comes from Higgs exchange via the mixing coupling λ.

4.1 Majorana mass splittings

Starting from the mass eigenstate basis in the minimal theory with Dirac fermions ψ_1 and ψ_2, it is convenient to re-express them in terms of their Weyl components as

$$\psi_1 = \begin{pmatrix} \chi_1 \\ \bar{\chi}_1^c \end{pmatrix}, \qquad \psi_2 = \begin{pmatrix} \chi_2 \\ \bar{\chi}_2^c \end{pmatrix}. \tag{4.2}$$

The mass matrix in the basis $(\chi_1, \chi_1^c, \chi_2, \chi_2^c)^t$ is then

$$\mathcal{M} = \begin{pmatrix} c_\alpha^2 M & m_1 & s_\alpha c_\alpha M & 0 \\ m_1 & c_\alpha^2 M & 0 & s_\alpha c_\alpha M \\ s_\alpha c_\alpha M & 0 & s_\alpha^2 M & m_2 \\ 0 & s_\alpha c_\alpha M & m_2 & s_\alpha^2 M \end{pmatrix}. \tag{4.3}$$

This matrix is diagonalized by the orthogonal transformation $\mathcal{O}$ given by

$$\mathcal{O} = \begin{pmatrix} \frac{1}{\sqrt{2}} & \frac{1}{\sqrt{2}} & 0 & 0 \\ -\frac{1}{\sqrt{2}} & \frac{1}{\sqrt{2}} & 0 & 0 \\ 0 & 0 & \frac{1}{\sqrt{2}} & \frac{1}{\sqrt{2}} \\ 0 & 0 & -\frac{1}{\sqrt{2}} & \frac{1}{\sqrt{2}} \end{pmatrix} \begin{pmatrix} i & 0 & 0 & 0 \\ 0 & 1 & 0 & 0 \\ 0 & 0 & i & 0 \\ 0 & 0 & 0 & 1 \end{pmatrix} \begin{pmatrix} c_{\gamma_-} & 0 & s_{\gamma_-} & 0 \\ 0 & c_{\gamma_+} & 0 & s_{\gamma_+} \\ -s_{\gamma_-} & 0 & c_{\gamma_-} & 0 \\ 0 & -s_{\gamma_+} & 0 & c_{\gamma_+} \end{pmatrix}, \tag{4.4}$$

such that $\mathcal{O}^t \mathcal{M} \mathcal{O} = \mathrm{diag}(m_{1_-}, m_{1_+}, m_{2_-}, m_{2_+})$ with

$$\begin{aligned} \tan(2\gamma_-) &= \frac{-\sin(2\alpha)\, M}{m_2 - m_1 + M\, \cos(2\alpha)}, \\ \tan(2\gamma_+) &= \frac{\sin(2\alpha)\, M}{m_2 - m_1 - M\, \cos(2\alpha)}, \end{aligned} \tag{4.5}$$

and mass eigenvalues

$$\begin{aligned} m_{1,2_-} &= \frac{1}{2}\left[m_1 + m_2 - M \mp \sqrt{(m_2 - m_1)^2 + 2(m_2 - m_1) M \cos(2\alpha) + M^2} \right], \\ m_{1,2_+} &= \frac{1}{2}\left[m_1 + m_2 + M \mp \sqrt{(m_2 - m_1)^2 - 2(m_2 - m_1) M \cos(2\alpha) + M^2} \right]. \end{aligned} \tag{4.6}$$

JHEP01(2023)014

For the specific and technically natural scenario of $M \ll m_2 - m_1$ that we focus on here, we have

$$\Delta m \equiv m_{1_+} - m_{1_-} \simeq 2\, M\, c_\alpha^2\,, \qquad m_{2_+} - m_{2_-} \simeq 2\, M\, s_\alpha^2\,, \tag{4.7}$$

together with

$$\gamma_\mp \simeq \mp s_\alpha c_\alpha \, \frac{M}{m_2 - m_1}\,, \tag{4.8}$$

corresponding to parametrically small Majorana mass splittings of would-be Dirac fermions.

Adding the additional mixing due to the Majorana mass to the interactions of the minimal theory, the terms relevant to our dark matter discussion are

$$\begin{aligned} -\mathscr{L} \supset & -\frac{\lambda}{2\sqrt{2}}\, \sin(2\alpha + 2\gamma_-)\, h\, \bar{\psi}_{1_-}\psi_{1_-} \\ & - i\, \bar{\psi}_{1_-}\gamma^\mu \psi_{1_+} \Big(\cos(\gamma_+ - \gamma_-)\, g_x\, X_\mu \; + [\cos(\gamma_+ - \gamma_-) - \cos(2\alpha + \gamma_+ + \gamma_-)]\, \frac{\bar{g}}{4}\, Z_\mu \Big)\,, \end{aligned} \tag{4.9}$$

where $\psi_{1_\mp} = (\chi_{1_\mp}, \bar{\chi}_{1_\mp})^t$ are the 4-component Majorana fermions constructed from χ_{1_-} and χ_{1_+}, and $\bar{g} = \sqrt{g^2 + g'^2}$. Here, we have only included Higgs terms involving ψ_{1_-} alone and dark vector couplings connecting ψ_{1_-} to ψ_{1_+}. Importantly, we note that there are no diagonal vector couplings between ψ_{1_-} and the vector bosons. This is enforced at tree-level by an approximate $\mathbb{Z}_2$ symmetry present when both Weyl components of N have equal Majorana mass terms M.[3] Moving away from this limit with $M_N \neq M_{N^c}$ allows diagonal vector couplings suppressed by at least one power of $(M_N - M_{N^c})/m_i \ll 1$.

4.2 Implications for dark matter

Dark matter freezeout with a parametrically small Majorana mass term proceeds as in the minimal Dirac theory provided $\Delta m \ll T_{fo} \sim m_1/25$, with approximately equal densities of ψ_{1_-} and ψ_{1_+} produced. The heavier ψ_{1_+} will then de-excite through decays via $\psi_{1_+} \to \psi_{1_-} + \{Z^*, X^*\}$ or by scattering with the cosmological bath [90, 91]. In the limit that $m_1,\, m_X \gg \Delta m \gg m_f$, the partial width to SM fermions $\psi_{1_+} \to \psi_{1_-} + f\bar{f}$ is

$$\begin{aligned} \Gamma_f &\simeq \frac{1}{60\pi^3} \left(a_f^2 + b_f^2\right) (\Delta m)^5 \\ &\simeq (9.0 \times 10^{-7}\,\mathrm{s})^{-1}\, \frac{(a_f^2 + b_f^2)}{G_F^2} \left(\frac{\Delta m}{100\ \mathrm{MeV}}\right)^5\,, \end{aligned} \tag{4.10}$$

while the thermally averaged scattering cross section for $\psi_{1_+} + f \to \psi_{1_-} + f$ de-excitation with $m_f \ll T \ll \Delta m$ is

$$\langle \sigma v \rangle \simeq \frac{1}{2\pi} \left(a_f^2 + b_f^2\right) (\Delta m)^2\,, \tag{4.11}$$

with

$$a_f \simeq -\frac{4\pi\, \epsilon\, \sqrt{\alpha\, \alpha_x}}{m_x^2} + \sqrt{2}\, G_F\, s_\alpha^2\, (t_f^3 - 2\, Q_f\, s_W^2)\,, \qquad b_f \simeq -\sqrt{2}\, G_F\, s_\alpha^2\, t_f^3\,, \tag{4.12}$$

[3] This symmetry is exact with only the connector and gauge sectors, but is broken by chiral SM matter.

where t_f^3 is the weak isospin of the left-handed fermion component and Q_f is the fermion electric charge. We find that the decays are typically rapid relative to the start of primordial nucleosynthesis ($\tau \lesssim 0.1\,\mathrm{s}$) for Δm larger than a few tens of MeV, and that de-excitation by scattering further depletes the heavier state. The resulting cosmological density of $\psi_{1\_}$ therefore matches that of ψ_1 computed previously in the minimal theory for appropriate values of $M \ll m_1$.

In contrast to freezeout, direct detection of $\psi_{1\_}$ dark matter is impacted very significantly by the Majorana mass splitting. This splitting leads to primarily off-diagonal $\psi_{1\_}$ gauge boson interactions involving the heavier fermions, thereby suppressing elastic vector exchange contributions to spin-independent (SI) scattering on nuclei. Inelastic scattering through vector exchange is still possible, but the rates for this process are very reduced or non-existent for a standard local DM halo velocity distribution and $\Delta m \gtrsim 200$–$500\,\mathrm{keV}$, depending on the target [88, 92]. The leading contribution to SI scattering then comes from Higgs boson exchange as described by the interactions of eq. (4.10). This coupling generates f_p and f_n coefficients of

$$f_p = -\tilde{d}_p \left(\frac{2}{9} + \frac{7}{9}\sum_q f_q^p\right), \qquad f_n = -\tilde{d}_n \left(\frac{2}{9} + \frac{7}{9}\sum_q f_q^n\right), \tag{4.13}$$

with

$$\tilde{d}_p = \tilde{d}_n = -\frac{m_n}{2v}\frac{\lambda \sin(2\alpha + 2\gamma_-)}{m_h^2}. \tag{4.14}$$

The effective SI cross section is given by eq. (3.1) with these coefficients.

In figure 4 we show the density-weighted SI per-nucleon cross section, $\sigma_{\mathrm{SI}}\,\rho_1/\rho_{\mathrm{DM}}$ in the extended theory of connector fermions with a Majorana mass. We assume that $m_2 - m_1 \gg \Delta m \gg 500\,\mathrm{keV}$ over the entire m_P–m_N plane and we set $\lambda = 0.1$ (top), $\lambda = 1.0$ (bottom), and $\alpha_x = \alpha$ (left) and $\alpha_x = 10\,\alpha$ (right). As before, the downward hatched regions show the exclusions from DM direct detection experiments, the solid black regions indicate where the $\psi_{1\_}$ relic density exceeds the observed DM density, and the grey regions denote exclusions from direct searches. As expected, the bounds from DM direct detection are significantly impacted by the Majorana mass. Even so, the remaining nucleon scattering mediated by Higgs exchange is significant and largely excluded by experiment unless the mixing between the singlet and doublet components is moderately small. This can be achieved for $\lambda \ll 1$, $m_P \ll m_N$, or $m_N \ll m_P$, and is directly analagous to the suppression of direct detection scattering for Higgsino-like dark matter in supersymmetry.

Beyond the exclusions shown in figure 4 from DM direct detection and the thermal overproduction of $\psi_{1\_}$, further restrictions on the parameter space can be derived from indirect DM searches such as gamma rays emitted from satellite galaxies [93] and the inner galaxy [94, 95], and distortions in the power spectra of the cosmic microwave background (CMB) [96–98]. In particular, for larger $\alpha_x \sim 10\,\alpha$ and $m_1 \gg m_x$ there can be a significant enhancement of the $\psi_{1\_}$ annihilation cross section at late times relative to freezeout due to the Sommerfeld effect and bound state formation [8, 9]. To estimate the enhancement relative to perturbative s-wave annihilation, we follow refs. [82, 83] and model the non-relativistic potential from dark vector boson exchange with a Hulthèn potential,

JHEP01(2023)014

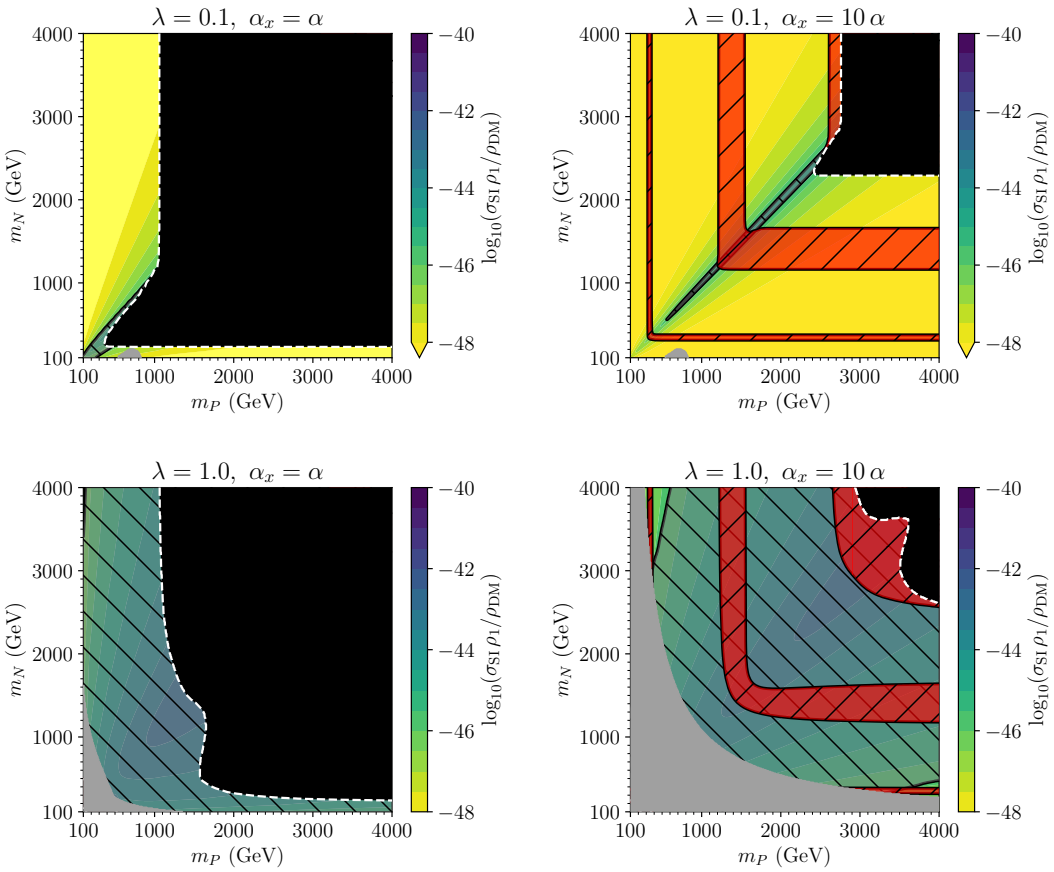

Figure 4. Contours of the density-weighted spin-independent per nucleon cross section $\sigma_{\rm SI}\,\rho_1/\rho_{\rm DM}$ for the Majorana extended theory in the m_P–m_N plane for $\lambda = 0.1,\ 1.0$ (top and bottom) and $\alpha_x = \alpha,\ 10\,\alpha$ (left and right). The downward hatched regions are excluded by DM direct detection searches, while the red upward hatched regions are ruled out by indirect detection tests. Also, the grey shaded regions show the combined exclusions from direct searches, and the black regions indicate where $\psi_{1\_}$ produces too much thermal dark matter.

which has been shown to give a good approximation for appropriate choices of parameters. Note that since we focus on parametrically small mass splittings, $\Delta m \ll m_x,\ m_1$, the Majorana mass is not expected to impact this result meaningfully [83].

We compare the enhanced cross sections for late-time $\psi_{1\_}$ annihilation computed this way to the bound on DM annihilation obtained from CMB observations by Planck [99]: $p_{\rm ann}({\rm DM}) \equiv f_{\rm ann}\,\langle\sigma v\rangle/m_{\rm DM} < p_{\rm ann}^{\rm lim} = 3.2\times10^{-28}\,{\rm cm}^3\,{\rm s}^{-1}\,{\rm GeV}^{-1}$, where $f_{\rm ann}$ is an efficiency factor that depends on the annihilation products and $\langle\sigma v\rangle$ is evaluated during recombination. This CMB bound is comparable to (but usually slightly weaker than) those from obtained gamma ray measurements [93], but it is also avoids potentially large astrophysical uncertainties. In evaluating $p_{\rm ann}(\psi_{1\_})$ for $\psi_{1\_}$ annihilation, we use a DM velocity of $v \sim \sqrt{0.3\,{\rm eV}/m_1}$ to estimate the non-perturbative enhancement factor and we fix $f_{\rm ann} = 0.2$ [100, 101]. We also rescale by the square of the fractional density of $\psi_{1\_}$ relative to dark matter and thus

JHEP01(2023)014

impose the requirement

$$p_{\rm ann}(\psi_{1_-}) < p_{\rm ann}^{\rm lim}\left(\frac{\rho_{\rm DM}}{\rho_1}\right)^2 . \tag{4.15}$$

The exclusions derived in this way are shown by the red upward hatched regions in figure 4. They appear only for larger dark gauge couplings $\alpha_x = 10\,\alpha$, and they exhibit a band structure corresponding to strong enhancement in specific regions through the formation of bound states. The locations of these exclusion bands depend on the mediator mass relative to the DM mass, but lie in a saturation regime that is largely insensitive to the DM velocity used in the calculuation provided it is small enough.

Finally, we emphasize that this extended connector theory can provide a viable dark matter candidate from the ψ_{1_-} state provided λ is not too large. This is demonstrated in the upper panels of figure 4 corresponding to $\lambda = 0.1$. The dashed white lines (at the boundaries of the parameter space excluded by the predicted relic density) indicate where ψ_{1_-} would make up all the DM. In the upper panels, we see that for $\lambda = 0.1$ these regions can also be consistent with limits from direct and indirect detection as well as laboratory tests of the theory. Depending on the relative sizes of m_P and m_N, this candidate is Higgsino-like ($m_P < m_N$) or secluded-DM-like ($m_P > m_N$).

4.3 Implications for direct searches

The Majorana mass term of eq. (4.1) requires the introduction of a new dark Higgs to the theory and modifies the spectrum relative to the minimal theory considered in section 2. We focus here on parametrically small mass splittings, $\Delta m \sim M = y_N \eta \ll m_x,\, m_1$, since they are sufficient to moderate dark matter direct detection. Given that $\eta = m_x/g_x$, this corresponds to the limit of $y_N \ll g_x$. With this hierarchy of couplings, the effect of the new operator need not significantly alter the non-dark matter phenomenology of the theory.

Starting with the dark Higgs itself, the new physical scalar φ obtained from $\Phi \to (\eta + \varphi/\sqrt{2})$ has efficient decays $\varphi \to X + X^{(*)}$ provided its mass is larger than the vector's, $m_\varphi \geq m_x$. We note, however, that for $m_\varphi < m_x$ the dark Higgs can be long-lived and potentially problematic for cosmology [47, 50, 102, 103]. The coupling of eq. (4.1) will also induce a Higgs portal operator $\lambda_{H\Phi}\, H^\dagger H\, \Phi^\dagger \Phi$ with $\lambda_{H\Phi} \sim \lambda^2 y_N^2 s_{2\alpha}^2/(4\pi)^2 \lesssim (\Delta m/m_x)^2 \alpha_x \lambda^2/4\pi$ through fermion loops, which is safely small for the $\Delta m/m_x \ll 1$ limit we focus on [15]. Moreover, with $y_N \ll g_x$ the impact of the dark Higgs on $\psi_{1_\mp}$ freezeout, annihilation, and direct detection is negligible.

In the limit of a parametrically small Majorana mass splitting among the fermions, the bounds from precision electroweak, Higgs decays, and direct collider searches will be essentially the same as found previously. As the mass splitting grows, a potentially interesting effect in collider searches is $\psi_{1_+} \to \psi_{1_-} + X^{(*)}$ at the end of decay cascades. These could appear in the multi-purpose LHC detectors [104] or in far detectors dedicated to long-lived particles [105–107].

JHEP01(2023)014

5 Decays through lepton mixing

A second approach to addressing the overabundance of relic portal fermions is to enable them to decay quickly enough to eliminate them as cosmological relics. Such decays can occur at the renormalizable level if there exists a dark Higgs field ϕ with dark charge $q_\phi = q_x$ that develops a VEV, $\langle\phi\rangle = \eta$. Such a field allows the P doublet to mix with the SM lepton doublets through the operator

$$-\mathscr{L} \supset \lambda_a \, \phi \, \overline{P}_R \, L_{La} + (\text{h.c.}) \,, \tag{5.1}$$

where $L_{La} = (1, 2, -1/2; 0)$ is the SM lepton doublet with flavor $a = e, \mu, \tau$. The cost of these interactions is that they can induce lepton flavour violation (LFV). In this section we show that the couplings of eq. (5.1) can allow ψ_1 to decay on cosmologically short timescales while not violating current bounds on LFV, even without imposing any particular flavour structure on the operators.

5.1 Charged lepton mixing

The interactions of eq. (5.1) mix the SM charged leptons with the P^- fermion. Working in a basis where the lepton Yukawa couplings are diagonal with $m_a = Y_a \langle H^0 \rangle$, the charged lepton mass terms take the form

$$-\mathscr{L} \supset \bar{\psi}^-_R \, M_\mp \, \psi^-_L + \text{h.c.} \,, \tag{5.2}$$

where $\psi^-_R = (P^-_R, e_{Ra})^t$, $\psi^-_L = (P^-_L, e_{La})^t$, and

$$M_\mp = \begin{pmatrix} m_P & \lambda_e \eta & \lambda_\mu \eta \\ 0 & m_e & 0 \\ 0 & 0 & m_\mu \end{pmatrix} . \tag{5.3}$$

Note that we have only written two SM generations here for brevity. The generalization to three generations is straightforward.

To diagonalize the charged mass matrix, we make the field transformations

$$\psi^-_L = U^\dagger \psi^{-\prime}_L \,, \qquad \psi_R = V^\dagger \psi^{-\prime}_R \,, \tag{5.4}$$

with unitary matrices U and V such that $VMU^\dagger = diag(m'_P, m'_e, m'_\mu)$. This implies that $VM_\mp M^\dagger_\mp V^\dagger = UM^\dagger_\mp M_\mp U^\dagger$. To linear order in the small quantities m_a/m_P, $\lambda_a \eta / m_P \ll 1$,

$$U^\dagger = \begin{pmatrix} 1 & -\lambda_e \eta/m_P & -\lambda_\mu \eta/m_P \\ \lambda_e \eta/m_P & 1 & 0 \\ \lambda_\mu \eta/m_P & 0 & 1 \end{pmatrix} + \mathcal{O}(\varepsilon^3) \,, \tag{5.5}$$

$$V^\dagger = \begin{pmatrix} 1 & -(\lambda_e \eta/m_P)^2 & -(\lambda_\mu \eta/m_P)^2 \\ (\lambda_e \eta/m_P)^2 & 1 & 0 \\ (\lambda_\mu \eta/m_P)^2 & 0 & 1 \end{pmatrix} + \mathcal{O}(\varepsilon^3) \,. \tag{5.6}$$

Furthermore, the mass matrix has two zero eigenvalues for m_e, $m_\mu \to 0$ implying $m'_a = m_a \, (1 + \mathcal{O}(\varepsilon^2))$ where ε denotes either m_a/m_P, $\lambda_a \eta / m_P \ll 1$, and thus the SM lepton masses remain proportional to their Yukawa couplings to the SM Higgs. The mass of the heavy state $P^{-\prime}$ also remains equal to m_P at this order.

JHEP01(2023)014

5.2 Neutral lepton mixing

The mass matrix for the neutral leptons is

$$-\mathscr{L} \supset \bar{\psi}^0_R M_0 \psi^0_L + h.c \tag{5.7}$$

where $\psi^0_R = (N^0_R, P^0_R)^t$, $\psi^0_L = (N^0_L, P^0_L, \nu_{L\,e}, \nu_{L\,\mu})^t$, and

$$M_0 = \begin{pmatrix} m_N & \lambda v & 0 & 0 \\ \lambda v & m_P & \lambda_e \eta & \lambda_\mu \eta \end{pmatrix}, \tag{5.8}$$

where again we show only the first two generations for brevity.

To find the mass eigenstates, we take

$$\psi^0_R = \mathcal{O}^\dagger B^\dagger \psi^{0\prime}_R\,, \qquad \psi^0_L = \begin{pmatrix} \mathcal{O}^\dagger & 0 \\ 0 & \mathbb{I} \end{pmatrix} A^\dagger \psi^{0\prime}_L\,, \tag{5.9}$$

where all matrices are unitary, and

$$\mathcal{O}^\dagger = \begin{pmatrix} c_\alpha & s_\alpha \\ -s_\alpha & c_\alpha \end{pmatrix} \tag{5.10}$$

corresponds to the mixing angles defined in eq. (2.2). This choice implies that as $\eta \to 0$ the matrices $A^\dagger$ and $B^\dagger$ vanish and the non-zero masses are m_1 and m_2 as before. These matrices can be found from the eigenvectors of $(B\mathcal{O})M_0 M_0^\dagger (\mathcal{O}^\dagger B^\dagger)$ for $B^\dagger$ and $(A\widetilde{\mathcal{O}})M_0^\dagger M_0 (\widetilde{\mathcal{O}}^\dagger A^\dagger)$ for $A^\dagger$. Expanding in the small quantities $\varepsilon = \lambda_a \eta / m_{1,2}$, we find $B^\dagger = \mathbb{I} + \mathcal{O}(\varepsilon^2)$ and

$$A^\dagger = \begin{pmatrix} \mathbb{I} & D^\dagger \\ -D & \mathbb{I} \end{pmatrix} + \mathcal{O}(\varepsilon^3)\,, \qquad D^\dagger = \begin{pmatrix} s_\alpha \lambda_e \eta / m_1 & s_\alpha \lambda_\mu \eta / m_1 \\ -c_\alpha \lambda_e \eta / m_2 & -c_\alpha \lambda_\mu \eta / m_2 \end{pmatrix}. \tag{5.11}$$

Based on the structure of these matrices, we are guaranteed to have two massless eigenvalues that we identify with the SM-like neutrinos. This implies that the new interaction of eq. (5.1) does not generate neutrino masses on its own and corrections to neutrino masses (necessarily from other sources) from the mixing are proportional to those masses. The non-zero mass eigenvalues remain m_1 and m_2 up to fractional corrections of order $\mathcal{O}(\varepsilon^2)$.

5.3 Interactions and heavy fermion decay

In appendix A, we collect the interactions between the new heavy fermions and the scalar and vector bosons of the SM, as well as the new lepton flavour mixing interactions between the SM fermions induced by the interaction of eq. (5.1). Expanding in powers of $\varepsilon \sim \{m_a, \lambda_a \eta\}/m_{1,2} \ll 1$, heavy-light lepton interactions arise at linear order in ε while LFV light-light lepton interactions are quadratic in ε. The lone exception to this comes from the interactions with the dark Higgs boson φ, obtained from $\phi \to (\eta + \varphi/\sqrt{2})$ in unitary gauge, which produce heavy-light fermion couplings at zeroeth order in ε.

Based on the structure of these couplings and counting powers of ε, the dominant ψ_1 decay channels would appear to be $\psi_1 \to \nu_{La} + \varphi$, with width

$$\Gamma(\psi_1 \to \nu_{La}\,\varphi) = \frac{\lambda_a^2 s_\alpha^2}{64\pi}\, m_1 \left[1 - \left(\frac{m_\varphi}{m_1}\right)^2\right]. \tag{5.12}$$

However, for $m_1 \gg m_x$ the decays $\psi_1 \to \nu_{La} + X^\mu$ receive a longitudinal enhancement,

$$\Gamma(\psi_1 \to \nu_{La}\, X) = \frac{\lambda_a^2 s_\alpha^2}{64\pi}\, m_1 \left[1 - \left(\frac{m_x}{m_1}\right)^2\right] \left[1 + 2\left(\frac{m_x}{m_1}\right)^2\right] . \tag{5.13}$$

In the limit $m_1 \gg m_\varphi, m_x$, the sum of these widths reproduces the width for $\psi_1 \to \nu_{La} + \phi$ in the $\mathrm{U}(1)_x$-unbroken theory, as expected from the Nambu-Goldstone equivalence theorem [108–110]. Relative to the decay channels involving φ or X^μ, all other modes are suppressed by factors of at least $(m_x/m_V)^2$, $\varepsilon^2 \ll 1$.

Using the decay widths above, the total lifetime of ψ_1 is

$$\tau \simeq (6.61 \times 10^{-8}\,\mathrm{s}) \left(\frac{10^{-9}}{\lambda_a s_\alpha}\right)^2 \left(\frac{\mathrm{TeV}}{m_1}\right) . \tag{5.14}$$

As long as the couplings are not exceedingly small, $\lambda_a s_\alpha \gtrsim 10^{-12}$, these decays occur before primordial nucleosynthesis and neutrino decoupling, and will generally be safe from cosmological bounds [111, 112]. Of course, this also eliminates ψ_1 as a relic particle and removes the bounds from direct detection since $\rho_1 \to 0$ today.

5.4 Lepton flavor mixing

The couplings collected in appendix A for this scenario give rise to lepton flavor violation (LFV) and modify leptonic anomalous magnetic moments $\Delta a_\ell \equiv a_\ell - a_\ell^{\mathrm{SM}}$. We compute here the new effects of the mixing from eq. (5.1) on Δa_ℓ and LFV observables [113–116].

In analogy to the decay calculation above, and counting powers of $\varepsilon \sim \lambda_a \eta / m_P \ll 1$, $(m_x/m_Z)^2 \ll 1$, the dominant new contributions to Δa_ℓ and LFV come from loop diagrams with the dark Higgs φ or the dark vector X^μ together with internal lines involving the heavy P^- fermion. For $m_P \gg m_\varphi, m_x$ the two contributions are approximately equal and sum to the result obtained by calculating in the $\mathrm{U}(1)_x$-unbroken theory provided $m_\phi \ll m_P$.

To see this explicitly, consider the leading contribution to the amplitude for $\ell_a(p) \to \ell_b(p') + \gamma(q)$ in the unbroken theory, corresponding to vertex and external leg diagrams with loops containing ϕ and P^-. We find

$$-i\mathcal{M}_{ab} \simeq \frac{i\, e\, \lambda_a \lambda_b^*}{32\,\pi^2}\, f(m_P, m_\phi)\, \bar{u}' i\sigma^{\mu\nu} q_\nu (m_b P_L + m_b P_R) u\, F_{\mu\nu} + (\ldots) , \tag{5.15}$$

where the omitted remainder is not relevant for Δa_μ or $\ell_a \to \ell_b + \gamma$ transitions, and the loop function $f(m_P, m_\phi)$ is

$$\begin{aligned} f(m_P, m_\phi) &= \int_0^1 dz \frac{z(1-z)^2}{(1-z)m_P^2 + z m_\phi^2} \\ &= \frac{1}{6m_\phi^2}\left[\frac{2 + 3r - 6r^2 + r^3 + 6r\ln r}{(1-r^4)}\right] \\ &\to \frac{1}{6m_P^2} \qquad (r \to \infty) , \end{aligned} \tag{5.16}$$

with $r = m_P^2/m_\phi^2$. Note that we have self-consistently neglected lepton masses $m_a \ll m_P$ beyond the leading non-trivial order and that our result matches refs. [113–115]. The

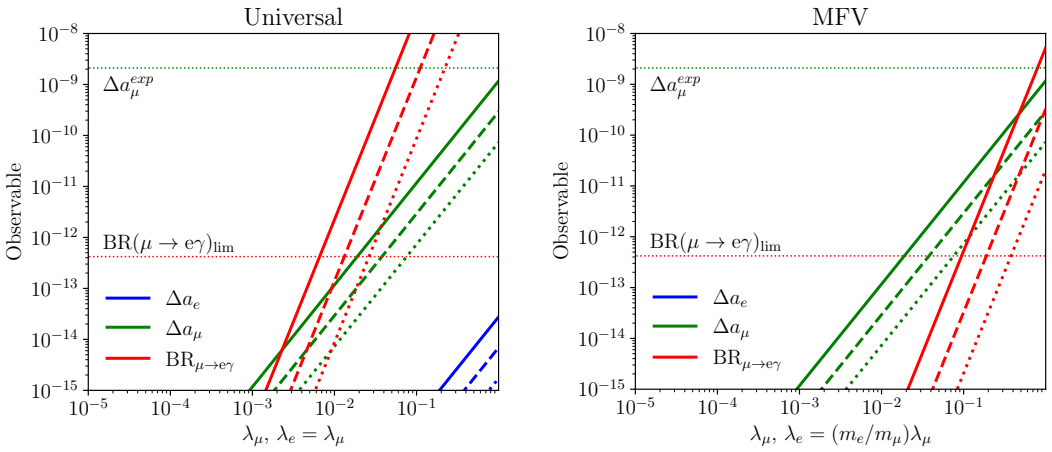

Figure 5. Charged lepton observables $\Delta a_{e,\mu}$ and $\mathrm{BR}(\mu \to e\gamma)$ in the lepton mixing model as a function of λ_μ assuming universal ($\lambda_e = \lambda_\mu$) or MFV-inspired ($\lambda_e = (m_e/m_\mu)\lambda_\mu$) couplings. For each observable, the solid, dashed, and dotted lines correspond to $m_P = 100, 200, 400$ GeV.

impact of m_P and m_ϕ is seen in the loop function, and eq. (5.16) shows that the result is independent of m_ϕ for $m_P^2 \gg m_\phi^2$ as claimed. We find the same leading result in the $\mathrm{U}(1)_x$-broken theory for $m_\varphi,\ m_x \ll m_P$.

Using eq. (5.15), we can extract the dominant contributions to Δa_ℓ as well as rates for $\ell_a \to \ell_b + \gamma$. For the first, we have

$$\Delta a_{\ell_a} = +\frac{\lambda_a^2}{96\pi^2}\left(\frac{m_a}{m_P}\right)^2 . \tag{5.17}$$

In turn, this can be related to the $\ell_a \to \ell_b + \gamma$ LFV rates by [115]

$$\mathrm{BR}(\mu \to e\gamma) = \frac{12\pi^3}{m_\mu^4}\frac{\alpha}{G_F^2}\left(\frac{\lambda_e}{\lambda_\mu}\right)^2 \times (\Delta a_\mu)^2, \tag{5.18}$$

$$\mathrm{BR}(\tau \to \mu\gamma) = \frac{12\pi^3}{m_\mu^4}\frac{\alpha}{G_F^2}\left(\frac{\lambda_\tau}{\lambda_\mu}\right)^2 \times (\Delta a_\mu)^2 \times \mathrm{BR}(\tau \to \mu\nu\bar{\nu})\,, \tag{5.19}$$

with $\mathrm{BR}(\tau \to \mu\nu\bar{\nu}) = 0.174$ [63].

In this theory the rates for $\ell_a \to \ell_b + \gamma$ also give a good proxy for other LFV observables. As an example, the amplitude for $\ell_a \to 3\ell_b$ has dipole and non-dipole contributions involving off-shell intermediate vector bosons that scale as $e\lambda_a\lambda_b$, as well as box contributions that go like $\lambda_a\lambda_b^3$. Since we focus on $\lambda_a \ll e,\ g_x$, the box diagrams are subleading relative to the off-shell vector contributions which have the same parametric dependence on the couplings as $\ell_a \to \ell_b + \gamma$. Put together, we expect $\mathrm{BR}(\ell_a \to 3\ell_b) \lesssim \alpha\,\mathrm{BR}(\ell_a \to \ell_b\gamma)$ [113, 114, 117]. A similar argument applies to $\mu N \to e N$ conversion. We also note that direct dark vector contributions to Δa_ℓ are negligible for the values $m_x = 15$ GeV and $|\epsilon| \lesssim 10^{-3}$ that we focus on [10].

In figure 5 we show the lepton mixing model predictions for the observables Δa_e (blue), Δa_μ (green), and $\mathrm{BR}(\mu \to e\gamma)$ (red) in terms of the coupling λ_μ for a universal scenario

JHEP01(2023)014

with $\lambda_e = \lambda_\mu$ (left) and a minimal flavour violation (MFV) inspired scenario with $\lambda_e = (m_e/m_\mu)\lambda_\mu$ (right). For all three observables, the solid lines correspond to $m_P = 100$ GeV, the dashed lines to $m_P = 200$ GeV, and the dotted lines to $m_P = 400$ GeV. The horizontal dotted lines indicate the combined experimental central value for $\Delta a_\mu = (2.51 \pm 0.59) \times 10^{-9}$ [118, 119] and the current bound on $\mathrm{BR}(\mu \to e\gamma) < 4.2 \times 10^{-13}$ [120]. We see from the figure that LFV provides the most stringent constraint on the lepton-mixing couplings λ_a, with $\lambda_\mu \lesssim 5 \times 10^{-3}$ sufficent for consistency with the current experimental result in the scenarios considered. Comparing to eq. (5.14), this implies that LFV bounds can easily be consistent with mediator fermion decays well before the era of primordial nucleosynthesis.

5.5 Other bounds

Lepton mixing in this scenario requires the presence of a new dark Higgs scalar φ. As in the Majorana mass scenario of section 4, the dark Higgs can be consistent with observations for $m_\varphi > m_x$ provided its Higgs portal coupling $\lambda_{\phi H}$ is not too large. Such a coupling will be induced by loops with $\lambda_{\phi H} \sim \lambda^2 \lambda_a^2/(4\pi)^2$ and are therefore naturally small for $\lambda_a \ll 1$.

Decays of the lightest connector fermion ψ_1 can change the collider signatures of the theory relative to the minimal model of section 2, where it is stable and produces missing energy. Collider events in this extension start out just like in the minimal theory, with dominant pair production of the connector fermions through Drell-Yan processes followed by cascade decays of the heavier states down to the lightest ψ_1 mode. However, ψ_1 now decays further to the SM through the dominant channels $\psi_1 \to \nu_a + \varphi$ and $\psi_1 \to \nu_a + X$. This yields additional visible energy from the subsequent $X \to f\bar{f}$ and $\varphi \to XX^{(*)}$ decays. Similar signals have been studied in supersymmetric dark sector models where the lightest SM superpartner decays to a lighter dark sector [8, 19, 102, 121–125].

If all the λ_a couplings are reasonably small, $\lambda_a s_\alpha \lesssim 10^{-10}$, eq. (5.14) implies that the ψ_1 is effectively stable with respect to standard collider detectors. Collider bounds on the theory are then the same as those discussed in section 2 with the ψ_1 producing missing energy. But in addition, the slow decays of this lightest connector fermion could potentially be observed at dedicated far detectors [105–107].

For larger couplings, ψ_1 can decay relatively promptly on typical collider timescales and generate additional visible energy in the events. In the limit $m_x \ll m_1$ the dark vector decay products will be at least moderately boosted and may give rise to lepton jets [8, 19]. These have been searched for in the context of Higgs boson decays to dark sector particles [126, 127] for both prompt [66, 67] and delayed dark particle decays [128, 129], but we do not know of a similar experimental analysis for production through connector fermions or supersymmetric cascades. Some insight into potential collider sensitivities can be obtained from LHC searches for heavy vector-like leptons that decay to taus or tau neutrinos. These produce events with Z, W, or h bosons together with additional visible energy from taus, instead of dark photons. These searches constrain doublet-like vector-like leptons up to masses approaching $m \gtrsim 1000$ GeV [130, 131] and suggest that similar bounds could be obtained on m_P in our lepton mixing scenario. We defer a detailed collider analysis of this scenario to a future work, as well as the impact on the sensitivity for intermediate mixing couplings that produce moderately long-lived ψ_1 fermions.

JHEP01(2023)014

6 Conclusions

In this work we have investigated the experimental and dark matter implications of matter connectors between the SM and a dark photon giving rise to kinetic mixing with hypercharge. Our focus was on a specific example of a dark $\mathrm{U}(1)_x$ gauge sector together with electroweak singlet and doublet Dirac connector fermions with gauge charges $N = (1, 1, 0; q_x)$ and $P = (1, 2, -1/2; q_x)$ that also couple to the SM Higgs field through a new Yukawa interaction. We expect that many of the conclusions we make for this particular theory apply to more general dark photon connectors.

In our example theory, electroweak symmetry breaking and the Higgs Yukawa leads to mixing between the fermions producing a lightest exotic state ψ_1. Without any further structure in the theory, gauge invariance implies that this fermion is stable and therefore contributes to the density of dark matter. We have studied the relic density ψ_1 obtains from thermal freezeout, as well as the signals it produces in dark matter search experiments. An acceptable relic density can be obtained provided it is not too heavy, $m_1 \lesssim 3$ TeV for reasonable couplings. However, being a Dirac fermion that couples to vector bosons, we find that the ψ_1 relic is nearly always ruled out by direct detection searches for dark matter, even when it only makes up a very small fraction of the total relic density.

To address this observational challenge to connector fermions that are light enough to have been produced thermally in the early universe, we investigated two extensions of the minimal theory. In the first, we introduced a dark Higgs field Φ with dark charge $q_\Phi = -2q_x$ that can give rise to a gauge-invariant Majorana mass term for ψ_1, splitting it into pseudo-Dirac components $\psi_{1_\mp}$. This eliminates the leading contributions to nucleon scattering from vector exchange and allows the relic to satisfy existing limits from direct detection. In fact, for a range of small mass splittings the ψ_{1_-} state can make up all the dark matter and be consistent with current experimental and observational bounds. In the second extension, we added a dark Higgs field ϕ with $q_\phi = q_x$ that allows the P fermion to mix with the SM lepton doublets. This induces decays of the lightest ψ_1 fermion to SM states but can also induce charged lepton flavour violation (LFV). We showed that the decays can be fast enough to be allowed by cosmology while also being consistent with tests of LFV.

Even though we have considered a specific example of connector fermions, similar considerations apply more generally to any new states carrying both SM and dark gauge charge. The lightest of these will be stable in the absence of dark symmetry breaking, and accidental flavor symmetries may lead to additional long-lived or stable states. When the dark gauge sector is Abelian, minimal mass terms for the connectors require Dirac or complex scalar representations (for $s < 1$ connectors), and their gauge charges lead to vector couplings to nucleons. These tend to produce nucleon scattering cross sections that are much larger than current limits, implying very strong constraints from direct detection if the connectors were created in the early Universe. Let us emphasize further that bounds on relic connectors will typically be even more stringent for other SM representations.

It is notable that the two solutions to this challenge that we have found both involve spontaneous Higgsing of the dark gauge group and are only possible for certain, specific

JHEP01(2023)014

gauge representations of the connector fermions. This has significant implications for the effective field theory describing dark photon interactions with the SM beyond the kinetic-mixing portal itself. Specifically, these points lead to the conclusion that combining the minimal connector theory with a Stueckelberg mechanism to generate the dark photon mass is inconsistent with a standard (hot) cosmological history. Thus, the need to associate the dark photon mass with the presence of a gauge symmetry informs the structure of higher-order operators allowed at the weak scale [132, 133] as well as the expected spectrum of states in the dark sector.

Acknowledgments

We thank Mary-Jean Harris for contributions at the beginning of this project. We also thank Hooman Davoudiasl, David McKeen, John Ng, and Nirmal Raj for helpful discussions. This work is supported by the Natural Sciences and Engineering Research Council of Canada (NSERC), with DM supported in part by a Discovery Grant. TRIUMF receives federal funding via a contribution agreement with the National Research Council of Canada.

A Interactions with lepton mixing

Relevant interactions in the minimal theory without lepton mixing are given in ref. [30]. Here, we extend these to include general lepton mixing terms of the form of eq. (5.1). The couplings of the minimal theory can also be obtained from these results by setting $\lambda_a = 0$.

The gauge and mass eigenstates involving the connector fermions are now $\psi^0_{L\,I} = (N^0_L, P^0_L, \nu_{L\,a})$, $\psi^0_{R\,i} = (N^0_R, P^0_R)$, $\psi^-_{L\,I} = (P^-_R, e_{L\,a})$, $\psi^-_{R\,I} = (P^-_R, e_{R\,a})$, where we label $I = i, a$, with $a = e, \mu, \tau$ and $i = (1), 2$. In the expressions below, we show the exact result in terms of the full mixing matrices as well as the leading non-trivial operators in powers of $\varepsilon = \lambda_a \eta / m_i \ll 1$.

Photon ($\Gamma = e\gamma^\mu A_\mu$)

$$\begin{aligned} -\mathscr{L} &\supset -\bar{\psi}^-_I \Gamma \psi^-_I \\ &= -\bar{\psi}^{-\prime}_I \Gamma \psi^{-\prime}_I \end{aligned} \tag{A.1}$$

Dark Photon ($\Gamma = g_x \gamma^\mu X_\mu$)

$$\begin{aligned} -\mathscr{L} &\supset \bar{\psi}^0_{L\,i} \Gamma \psi^0_{L\,i} + \bar{\psi}^0_{R\,i} \Gamma \psi^0_{R\,i} + \bar{\psi}^-_{L\,i} \Gamma \psi^-_{L\,i} + \bar{\psi}^-_{R\,i} \Gamma \psi^-_{R\,i} \\ &= \bar{\psi}^{0\prime}_{L\,I} \Gamma (A\widetilde{\mathcal{O}})_{Ii} (\widetilde{\mathcal{O}}^\dagger A^\dagger)_{iJ} \psi^{0\prime}_{L\,J} + \bar{\psi}^{0\prime}_{R\,i} \Gamma \psi^{0\prime}_{R\,i} \\ &\quad + \bar{\psi}^{-\prime}_{L\,I} \Gamma U_{Ii} U^\dagger_{iJ} \psi^{-\prime}_{L\,J} + \bar{\psi}^{-\prime}_{R\,i} \Gamma V_{Ii} V^\dagger_{iJ} \psi^{-\prime}_{R\,i} \\ &\simeq \bar{\psi}^{0\prime}_{Li} \Gamma \psi^{0\prime}_{Li} + \bar{\psi}^{0\prime}_{Ri} \Gamma \psi^{0\prime}_{Ri} \\ &\quad + \lambda_a \eta \left[\left(-\frac{s_\alpha}{m_1} \bar{\psi}^{0\prime}_{L1} + \frac{c_\alpha}{m_2} \bar{\psi}^{0\prime}_{L2} \right) \Gamma \nu'_{La} + \text{h.c.} \right] - \lambda_a \lambda_b \eta^2 \left(\frac{s^2_\alpha}{m^2_1} + \frac{c^2_\alpha}{m^2_2} \right) \bar{\nu}'_{La} \Gamma \nu'_{Lb} \\ &\quad + \bar{\psi}^{-\prime}_{Li} \Gamma \psi^{-\prime}_{Li} + \bar{\psi}^{-\prime}_{Ri} \Gamma \psi^{-\prime}_{Ri} - \left[\bar{\psi}^{-\prime}_{Li} \Gamma \left(\lambda_a \eta / m_P \right) e'_{La} + \text{h.c.} \right] + \bar{e}'_{La} \Gamma \left(\lambda_a \lambda_b \eta^2 / m^2_P \right) e'_{Lb} \end{aligned} \tag{A.2}$$

JHEP01(2023)014

Z Boson ($\boldsymbol{\Gamma = \frac{g}{c_W}\gamma^\mu Z_\mu}$)

$$
\begin{aligned}
-\mathscr{L} \supset\ & \frac{1}{2}\bar{\psi}^0_{LI}\Gamma(\delta_{IJ}-\delta_{I1}\delta_{1J})\psi^0_{LI} + \frac{1}{2}\bar{\psi}^0_{Ri}\Gamma\delta_{i2}\delta_{2j}\psi^0_{Ri} \\
& + \left(-\frac{1}{2}+s_W^2\right)\bar{\psi}^-_{LI}\Gamma\delta_{IJ}\psi^-_{LJ} + \bar{\psi}^-_{RI}\Gamma\left(s_W^2\delta_{IJ}-\frac{1}{2}\delta_{I2}\delta_{2J}\right)\psi^-_{RJ} \\
=\ & \frac{1}{2}\bar{\psi}^{0\prime}_{LI}\Gamma[\delta_{IJ}-(A\widetilde{O})_{I1}(\widetilde{O}^\dagger A^\dagger)_{1J}]\psi^{0\prime}_{LJ} + \frac{1}{2}\bar{\psi}^{0\prime}_{Ri}\Gamma[(B\mathcal{O})_{i2}(\mathcal{O}^\dagger B^\dagger)_{2j}]\psi^{0\prime}_{Rj} \\
& + \left(-\frac{1}{2}+s_W^2\right)\bar{\psi}^{-\prime}_{LI}\Gamma\,\delta_{IJ}\,\psi^{-\prime}_{LJ} + \bar{\psi}^{-\prime}_{RI}\Gamma\left(s_W^2\delta_{IJ}-\frac{1}{2}V_{I2}V^\dagger_{2J}\right)\psi^{-\prime}_{RJ} \\
\simeq\ & \frac{1}{2}[s_\alpha^2\bar{\psi}^{0\prime}_1\Gamma\psi^{0\prime}_1 + c_\alpha^2\bar{\psi}^{0\prime}_2\Gamma\psi^{0\prime}_2 - c_\alpha s_\alpha(\bar{\psi}^{0\prime}_1\Gamma\psi^{0\prime}_2+\text{h.c.})] \\
& + \left(-\frac{1}{2}+s_W^2\right)P^{-\prime}\Gamma P^{-\prime} + \left(-\frac{1}{2}+s_W^2\right)e'_{La}\Gamma e'_{La} + s_W^2\bar{e}'_{Ra}\Gamma e'_{Ra} \\
& - \lambda_a c_\alpha s_\alpha\eta\left(\frac{m_2-m_1}{m_1m_2}\right)(c_\alpha\bar{\psi}'_{1L}+s_\alpha\bar{\psi}'_{2L})\Gamma\nu'_{La}+\text{h.c.} \\
& - \lambda_a\lambda_b\eta^2 s_\alpha^2 c_\alpha^2\left(\frac{m_2-m_1}{m_1m_2}\right)^2\bar{e}'_{La}\Gamma e'_{Lb}\,.
\end{aligned}
\tag{A.3}
$$

W Boson ($\boldsymbol{\Gamma = \frac{g}{\sqrt{2}}\gamma^\mu W_\mu}$)

$$
\begin{aligned}
-\mathscr{L} \supset\ & \bar{\psi}^-_{LI'}\Gamma\psi^0_{LI'} + \bar{\psi}^-_{RI'}\Gamma\delta_{I'2}\delta_{2j}\psi^0_{Rj} + \text{h.c.} \\
=\ & \bar{\psi}^{-\prime}_{LI'}\Gamma U_{I'K'}(\mathcal{O}^\dagger A^\dagger)_{K'J}\psi^{0\prime}_{LJ} + \bar{\psi}^{-\prime}_{RI'}\Gamma V_{I'2}(\mathcal{O}^\dagger B^\dagger)_{2j}\psi^{0\prime}_{Rj} + \text{h.c.} \\
=\ & \bar{P}^{-\prime}\Gamma(-s_\alpha\psi^{0\prime}_1 + c_\alpha\psi^{0\prime}_2) + \bar{e}'_{La}\Gamma\nu_{La} \\
& - \lambda_a\eta\left(\frac{1}{m_P}+\frac{s_\alpha^2}{m_1}+\frac{c_\alpha^2}{m_2}\right)\bar{P}^{-\prime}_L\Gamma\nu_{La} - \frac{\lambda_a\eta}{m_P}\bar{e}'_{La}\Gamma(-s_\alpha\psi^{0\prime}_{L1}+c_\alpha\psi^{0\prime}_{L2}) \\
& + \frac{\lambda_a\lambda_b\,\eta^2}{m_P}\left(\frac{s_\alpha^2}{m_1}+\frac{c_\alpha^2}{m_2}\right)\bar{e}'_{La}\Gamma\nu'_{Lb}+\text{h.c.}
\end{aligned}
\tag{A.4}
$$

Higgs Boson ($\boldsymbol{\Gamma = h/\sqrt{2}}$)

$$
\begin{aligned}
-\mathscr{L} \supset\ & Y_a\,\bar{\psi}^-_{RI}\Gamma\delta_{Ia}\delta_{aJ}\psi_{LJ} + \lambda\,\bar{\psi}^0_{Ri}\Gamma\,(\delta_{i1}\delta_{2J}+\delta_{i2}\delta_{1J})\,\psi^-_{LJ} + \text{h.c.} \\
=\ & Y_a\,\bar{\psi}^-_{RI}\Gamma V_{Ia}U^\dagger_{aJ}\psi_{LJ} + \lambda\,\bar{\psi}^0_{Ri}\Gamma\left[(B\mathcal{O})_{i1}(\mathcal{O}^\dagger A^\dagger)_{2J} + (B\mathcal{O})_{i2}(\mathcal{O}^\dagger A^\dagger)_{1J}\right]\psi^{0\prime}_{LJ} + \text{h.c.} \\
\simeq\ & Y_a\,\bar{e}'_{Ra}\Gamma e'_{La} + Y_a\,\frac{\lambda_a\eta}{m_P}\,\bar{e}'_{Ra}\Gamma P^{-\prime}_L \\
& \lambda\,s_{2\alpha}\left(-\bar{\psi}^{0\prime}_{1R}\Gamma\psi^{0\prime}_{1L} + \bar{\psi}^{0\prime}_{2R}\Gamma\psi^{0\prime}_{2L}\right) + \lambda\,c_{2\alpha}\left(\bar{\psi}^{0\prime}_{1R}\Gamma\psi^{0\prime}_{2L} + \bar{\psi}^{0\prime}_{2R}\Gamma\psi^{0\prime}_{1L}\right) \\
& - \lambda\,\lambda_a\eta\left(s_{2\alpha}\frac{s_\alpha}{m_1}+c_{2\alpha}\frac{c_\alpha}{m_2}\right)\bar{\psi}^{0\prime}_{1R}\Gamma\nu'_{La} + \lambda\,\lambda_a\eta\left(c_{2\alpha}\frac{s_\alpha}{m_1}-s_{2\alpha}\frac{c_\alpha}{m_2}\right)\bar{\psi}^{0\prime}_{2R}\Gamma\nu'_{La}+\text{h.c.}
\end{aligned}
\tag{A.5}
$$

JHEP01(2023)014

Dark Higgs Boson ($\Gamma = \varphi/\sqrt{2}$)

$$
\begin{aligned}
-\mathscr{L} \supset\ & \bar{\psi}^{-}_{RI}\Gamma(\delta_{I2}\lambda_a\delta_{aJ})\psi^{-}_{LJ} + \bar{\psi}^{0}_{Ri}\Gamma(\delta_{i2}\lambda_a\delta_{aJ})\psi^{0}_{LJ} \\
=\ & \bar{\psi}^{-\prime}_{RI}\Gamma(V_{I2}\lambda_a U^{\dagger}_{aJ})\psi^{-}_{LJ} + \bar{\psi}^{0}_{Ri}\Gamma[(B\mathcal{O})_{i2}\lambda_a(\tilde{\mathcal{O}}^{\dagger}A^{\dagger})_{aJ}]\psi^{0}_{LJ} \\
\simeq\ & \lambda_a \bar{P}^{-\prime}_{R}\Gamma e'_{La} + \frac{\lambda_a^2\eta}{m_P}\bar{P}^{-\prime}_{R}\Gamma\bar{P}^{-\prime}_{L} - \frac{\lambda_a\lambda_b^2\eta^2}{m_P^2}\bar{e}'_{Rb}\Gamma e'_{La} \\
& + \lambda_a\left(-s_\alpha\bar{\psi}^{0\prime}_{R1} + c_\alpha\bar{\psi}^{0\prime}_{R2}\right)\Gamma\nu_{La} \\
& + \lambda_c^2\eta(-s_\alpha\bar{\psi}^{0\prime}_{R1} + c_\alpha\bar{\psi}^{0\prime}_{R2})\Gamma\left(-\frac{s_\alpha}{m_1}\psi^{0\prime}_{L1} + \frac{c_\alpha}{m_2}\psi^{0\prime}_{L2}\right) + \text{h.c.}
\end{aligned}
\tag{A.6}
$$

References

[1] J.L. Hewett and T.G. Rizzo, *Low-Energy Phenomenology of Superstring Inspired E_6 Models*, *Phys. Rept.* **183** (1989) 193 [INSPIRE].

[2] G. Aldazabal, S. Franco, L.E. Ibanez, R. Rabadan and A.M. Uranga, *Intersecting brane worlds*, *JHEP* **02** (2001) 047 [hep-ph/0011132] [INSPIRE].

[3] R. Blumenhagen, B. Kors, D. Lust and S. Stieberger, *Four-dimensional String Compactifications with D-Branes, Orientifolds and Fluxes*, *Phys. Rept.* **445** (2007) 1 [hep-th/0610327] [INSPIRE].

[4] P. Langacker, *The Physics of Heavy Z' Gauge Bosons*, *Rev. Mod. Phys.* **81** (2009) 1199 [arXiv:0801.1345] [INSPIRE].

[5] C. Boehm and P. Fayet, *Scalar dark matter candidates*, *Nucl. Phys. B* **683** (2004) 219 [hep-ph/0305261] [INSPIRE].

[6] N. Borodatchenkova, D. Choudhury and M. Drees, *Probing MeV dark matter at low-energy e+e- colliders*, *Phys. Rev. Lett.* **96** (2006) 141802 [hep-ph/0510147] [INSPIRE].

[7] M. Pospelov, A. Ritz and M.B. Voloshin, *Secluded WIMP Dark Matter*, *Phys. Lett. B* **662** (2008) 53 [arXiv:0711.4866] [INSPIRE].

[8] N. Arkani-Hamed, D.P. Finkbeiner, T.R. Slatyer and N. Weiner, *A Theory of Dark Matter*, *Phys. Rev. D* **79** (2009) 015014 [arXiv:0810.0713] [INSPIRE].

[9] M. Pospelov and A. Ritz, *Astrophysical Signatures of Secluded Dark Matter*, *Phys. Lett. B* **671** (2009) 391 [arXiv:0810.1502] [INSPIRE].

[10] M. Pospelov, *Secluded* U(1) *below the weak scale*, *Phys. Rev. D* **80** (2009) 095002 [arXiv:0811.1030] [INSPIRE].

[11] J.D. Bjorken, R. Essig, P. Schuster and N. Toro, *New Fixed-Target Experiments to Search for Dark Gauge Forces*, *Phys. Rev. D* **80** (2009) 075018 [arXiv:0906.0580] [INSPIRE].

[12] L.B. Okun, *Limits of electrodynamics: paraphotons?*, *Sov. Phys. JETP* **56** (1982) 502 [INSPIRE].

[13] B. Holdom, *Two* U(1)*'s and Epsilon Charge Shifts*, *Phys. Lett. B* **166** (1986) 196 [INSPIRE].

JHEP01(2023)014

[14] G. Lanfranchi, M. Pospelov and P. Schuster, *The Search for Feebly Interacting Particles*, *Ann. Rev. Nucl. Part. Sci.* **71** (2021) 279 [arXiv:2011.02157] [INSPIRE].

[15] P. Agrawal et al., *Feebly-interacting particles: FIPs 2020 workshop report*, *Eur. Phys. J. C* **81** (2021) 1015 [arXiv:2102.12143] [INSPIRE].

[16] J. Alexander et al., *Dark Sectors 2016 Workshop: Community Report*, arXiv:1608.08632 [INSPIRE].

[17] B. Batell, N. Blinov, C. Hearty and R. McGehee, *Exploring Dark Sector Portals with High Intensity Experiments*, in *2022 Snowmass Summer Study*, arXiv:2207.06905 [INSPIRE].

[18] G. Krnjaic et al., *A Snowmass Whitepaper: Dark Matter Production at Intensity-Frontier Experiments*, arXiv:2207.00597 [INSPIRE].

[19] N. Arkani-Hamed and N. Weiner, *LHC Signals for a SuperUnified Theory of Dark Matter*, *JHEP* **12** (2008) 104 [arXiv:0810.0714] [INSPIRE].

[20] T. Gherghetta, J. Kersten, K. Olive and M. Pospelov, *Evaluating the price of tiny kinetic mixing*, *Phys. Rev. D* **100** (2019) 095001 [arXiv:1909.00696] [INSPIRE].

[21] K. Griest and M. Kamionkowski, *Unitarity Limits on the Mass and Radius of Dark Matter Particles*, *Phys. Rev. Lett.* **64** (1990) 615 [INSPIRE].

[22] B.W. Lee and S. Weinberg, *Cosmological Lower Bound on Heavy Neutrino Masses*, *Phys. Rev. Lett.* **39** (1977) 165 [INSPIRE].

[23] M.L. Perl, E.R. Lee and D. Loomba, *Searches for fractionally charged particles*, *Ann. Rev. Nucl. Part. Sci.* **59** (2009) 47 [INSPIRE].

[24] V. De Luca, A. Mitridate, M. Redi, J. Smirnov and A. Strumia, *Colored Dark Matter*, *Phys. Rev. D* **97** (2018) 115024 [arXiv:1801.01135] [INSPIRE].

[25] G. Jungman, M. Kamionkowski and K. Griest, *Supersymmetric dark matter*, *Phys. Rept.* **267** (1996) 195 [hep-ph/9506380] [INSPIRE].

[26] E. Del Nobile, *The Theory of Direct Dark Matter Detection: A Guide to Computations*, arXiv:2104.12785 [INSPIRE].

[27] LZ collaboration, *First Dark Matter Search Results from the LUX-ZEPLIN (LZ) Experiment*, arXiv:2207.03764 [INSPIRE].

[28] H. Davoudiasl, H.-S. Lee and W.J. Marciano, *Dark Side of Higgs Diphoton Decays and Muon g-2*, *Phys. Rev. D* **86** (2012) 095009 [arXiv:1208.2973] [INSPIRE].

[29] J.M. Cline, J.M. Cornell, D. London and R. Watanabe, *Hidden sector explanation of B-decay and cosmic ray anomalies*, *Phys. Rev. D* **95** (2017) 095015 [arXiv:1702.00395] [INSPIRE].

[30] Q. Lu, D.E. Morrissey and A.M. Wijangco, *Higgs Boson Decays to Dark Photons through the Vectorized Lepton Portal*, *JHEP* **06** (2017) 138 [arXiv:1705.08896] [INSPIRE].

[31] A. Azatov, J. Galloway and M.A. Luty, *Superconformal Technicolor*, *Phys. Rev. Lett.* **108** (2012) 041802 [arXiv:1106.3346] [INSPIRE].

[32] J.J. Heckman, P. Kumar, C. Vafa and B. Wecht, *Electroweak Symmetry Breaking in the DSSM*, *JHEP* **01** (2012) 156 [arXiv:1108.3849] [INSPIRE].

[33] P.W. Graham, D.E. Kaplan and S. Rajendran, *Cosmological Relaxation of the Electroweak Scale*, *Phys. Rev. Lett.* **115** (2015) 221801 [arXiv:1504.07551] [INSPIRE].

JHEP01(2023)014

[34] H. Beauchesne, E. Bertuzzo and G. Grilli di Cortona, *Constraints on the relaxion mechanism with strongly interacting vector-fermions*, *JHEP* **08** (2017) 093 [arXiv:1705.06325] [INSPIRE].

[35] G.N. Wojcik and T.G. Rizzo, SU(4) *flavorful portal matter*, *Phys. Rev. D* **105** (2022) 015032 [arXiv:2012.05406] [INSPIRE].

[36] T.G. Rizzo, *Toward a UV model of kinetic mixing and portal matter. II. Exploring unification in an SU(N) group*, *Phys. Rev. D* **106** (2022) 095024 [arXiv:2209.00688] [INSPIRE].

[37] J.M. Cline, W. Huang and G.D. Moore, *Challenges for models with composite states*, *Phys. Rev. D* **94** (2016) 055029 [arXiv:1607.07865] [INSPIRE].

[38] C.D. Carone, S. Chaurasia and T.V.B. Claringbold, *Dark sector portal with vectorlike leptons and flavor sequestering*, *Phys. Rev. D* **99** (2019) 015009 [arXiv:1807.05288] [INSPIRE].

[39] T.G. Rizzo, *Kinetic Mixing and Portal Matter Phenomenology*, *Phys. Rev. D* **99** (2019) 115024 [arXiv:1810.07531] [INSPIRE].

[40] J.H. Kim, S.D. Lane, H.-S. Lee, I.M. Lewis and M. Sullivan, *Searching for Dark Photons with Maverick Top Partners*, *Phys. Rev. D* **101** (2020) 035041 [arXiv:1904.05893] [INSPIRE].

[41] J.M. Lamprea, E. Peinado, S. Smolenski and J. Wudka, *Self-interacting neutrino portal dark matter*, *Phys. Rev. D* **103** (2021) 015017 [arXiv:1906.02340] [INSPIRE].

[42] T.D. Rueter and T.G. Rizzo, *Towards A UV-Model of Kinetic Mixing and Portal Matter*, *Phys. Rev. D* **101** (2020) 015014 [arXiv:1909.09160] [INSPIRE].

[43] R. Coy and T. Hambye, *Neutrino lines from DM decay induced by high-scale seesaw interactions*, *JHEP* **05** (2021) 101 [arXiv:2012.05276] [INSPIRE].

[44] M. Cirelli, N. Fornengo and A. Strumia, *Minimal dark matter*, *Nucl. Phys. B* **753** (2006) 178 [hep-ph/0512090] [INSPIRE].

[45] M. Kawasaki, K. Kohri, T. Moroi and Y. Takaesu, *Revisiting Big-Bang Nucleosynthesis Constraints on Long-Lived Decaying Particles*, *Phys. Rev. D* **97** (2018) 023502 [arXiv:1709.01211] [INSPIRE].

[46] T.R. Slatyer and C.-L. Wu, *General Constraints on Dark Matter Decay from the Cosmic Microwave Background*, *Phys. Rev. D* **95** (2017) 023010 [arXiv:1610.06933] [INSPIRE].

[47] B. Batell, M. Pospelov and A. Ritz, *Probing a Secluded* U(1) *at B-factories*, *Phys. Rev. D* **79** (2009) 115008 [arXiv:0903.0363] [INSPIRE].

[48] R. Essig, P. Schuster and N. Toro, *Probing Dark Forces and Light Hidden Sectors at Low-Energy e^+e^- Colliders*, *Phys. Rev. D* **80** (2009) 015003 [arXiv:0903.3941] [INSPIRE].

[49] P. Schuster, N. Toro and I. Yavin, *Terrestrial and Solar Limits on Long-Lived Particles in a Dark Sector*, *Phys. Rev. D* **81** (2010) 016002 [arXiv:0910.1602] [INSPIRE].

[50] D.E. Morrissey and A.P. Spray, *New Limits on Light Hidden Sectors from Fixed-Target Experiments*, *JHEP* **06** (2014) 083 [arXiv:1402.4817] [INSPIRE].

[51] BELLE collaboration, *Search for the dark photon and the dark Higgs boson at Belle*, *Phys. Rev. Lett.* **114** (2015) 211801 [arXiv:1502.00084] [INSPIRE].

[52] L. Darmé, S. Rao and L. Roszkowski, *Light dark Higgs boson in minimal sub-GeV dark matter scenarios*, *JHEP* **03** (2018) 084 [arXiv:1710.08430] [INSPIRE].

[53] I. Banta, T. Cohen, N. Craig, X. Lu and D. Sutherland, *Non-decoupling new particles*, *JHEP* **02** (2022) 029 [arXiv:2110.02967] [INSPIRE].

JHEP01(2023)014

[54] E.C.G. Stueckelberg, *Theory of the radiation of photons of small arbitrary mass*, *Helv. Phys. Acta* **30** (1957) 209 [INSPIRE].

[55] B. Kors and P. Nath, *A Stueckelberg extension of the standard model*, *Phys. Lett. B* **586** (2004) 366 [hep-ph/0402047] [INSPIRE].

[56] A. DiFranzo, P.J. Fox and T.M.P. Tait, *Vector Dark Matter through a Radiative Higgs Portal*, *JHEP* **04** (2016) 135 [arXiv:1512.06853] [INSPIRE].

[57] A. DiFranzo and G. Mohlabeng, *Multi-component Dark Matter through a Radiative Higgs Portal*, *JHEP* **01** (2017) 080 [arXiv:1610.07606] [INSPIRE].

[58] M.A. Shifman, A.I. Vainshtein, M.B. Voloshin and V.I. Zakharov, *Low-Energy Theorems for Higgs Boson Couplings to Photons*, *Sov. J. Nucl. Phys.* **30** (1979) 711 [INSPIRE].

[59] LHCb collaboration, *Search for $A' \to \mu^+\mu^-$ Decays*, *Phys. Rev. Lett.* **124** (2020) 041801 [arXiv:1910.06926] [INSPIRE].

[60] CMS collaboration, *Search for a Narrow Resonance Lighter than 200 GeV Decaying to a Pair of Muons in Proton-Proton Collisions at $\sqrt{s} =$ TeV*, *Phys. Rev. Lett.* **124** (2020) 131802 [arXiv:1912.04776] [INSPIRE].

[61] M.E. Peskin and T. Takeuchi, *A new constraint on a strongly interacting Higgs sector*, *Phys. Rev. Lett.* **65** (1990) 964 [INSPIRE].

[62] M.E. Peskin and T. Takeuchi, *Estimation of oblique electroweak corrections*, *Phys. Rev. D* **46** (1992) 381 [INSPIRE].

[63] Particle Data Group collaboration, *Review of Particle Physics*, *PTEP* **2020** (2020) 083C01 [INSPIRE].

[64] CDF collaboration, *High-precision measurement of the W boson mass with the CDF II detector*, *Science* **376** (2022) 170 [INSPIRE].

[65] ATLAS collaboration, *Search for invisible Higgs-boson decays in events with vector-boson fusion signatures using 139 fb^{-1} of proton-proton data recorded by the ATLAS experiment*, *JHEP* **08** (2022) 104 [arXiv:2202.07953] [INSPIRE].

[66] ATLAS collaboration, *Search for Higgs bosons decaying into new spin-0 or spin-1 particles in four-lepton final states with the ATLAS detector with 139 fb^{-1} of pp collision data at $\sqrt{s} = 13$ TeV*, *JHEP* **03** (2022) 041 [arXiv:2110.13673] [INSPIRE].

[67] CMS collaboration, *Search for low-mass dilepton resonances in Higgs boson decays to four-lepton final states in proton-proton collisions at $\sqrt{s} = 13$ TeV*, *Eur. Phys. J. C* **82** (2022) 290 [arXiv:2111.01299] [INSPIRE].

[68] D. Curtin, R. Essig, S. Gori and J. Shelton, *Illuminating Dark Photons with High-Energy Colliders*, *JHEP* **02** (2015) 157 [arXiv:1412.0018] [INSPIRE].

[69] A. Canepa, T. Han and X. Wang, *The Search for Electroweakinos*, *Ann. Rev. Nucl. Part. Sci.* **70** (2020) 425 [arXiv:2003.05450] [INSPIRE].

[70] T. Cohen, J. Kearney, A. Pierce and D. Tucker-Smith, *Singlet-Doublet Dark Matter*, *Phys. Rev. D* **85** (2012) 075003 [arXiv:1109.2604] [INSPIRE].

[71] T.A.W. Martin and D. Morrissey, *Electroweakino constraints from LHC data*, *JHEP* **12** (2014) 168 [arXiv:1409.6322] [INSPIRE].

[72] J. Liu, N. McGinnis, C.E.M. Wagner and X.-P. Wang, *Searching for the Higgsino-Bino Sector at the LHC*, *JHEP* **09** (2020) 073 [arXiv:2006.07389] [INSPIRE].

JHEP01(2023)014

[73] ATLAS collaboration, *Search for charginos and neutralinos in final states with two boosted hadronically decaying bosons and missing transverse momentum in pp collisions at $\sqrt{s} = 13$ TeV with the ATLAS detector*, *Phys. Rev. D* **104** (2021) 112010 [arXiv:2108.07586] [INSPIRE].

[74] J. Alwall et al., *The automated computation of tree-level and next-to-leading order differential cross sections, and their matching to parton shower simulations*, *JHEP* **07** (2014) 079 [arXiv:1405.0301] [INSPIRE].

[75] A. Alloul, N.D. Christensen, C. Degrande, C. Duhr and B. Fuks, *FeynRules 2.0 — A complete toolbox for tree-level phenomenology*, *Comput. Phys. Commun.* **185** (2014) 2250 [arXiv:1310.1921] [INSPIRE].

[76] G. Cowan, K. Cranmer, E. Gross and O. Vitells, *Asymptotic formulae for likelihood-based tests of new physics*, *Eur. Phys. J. C* **71** (2011) 1554 [arXiv:1007.1727] [INSPIRE].

[77] N.D. Christensen and C. Duhr, *FeynRules — Feynman rules made easy*, *Comput. Phys. Commun.* **180** (2009) 1614 [arXiv:0806.4194] [INSPIRE].

[78] C. Degrande, C. Duhr, B. Fuks, D. Grellscheid, O. Mattelaer and T. Reiter, *UFO — The Universal FeynRules Output*, *Comput. Phys. Commun.* **183** (2012) 1201 [arXiv:1108.2040] [INSPIRE].

[79] M. Backović, K. Kong and M. McCaskey, *MadDM v.1.0: Computation of Dark Matter Relic Abundance Using MadGraph5*, *Physics of the Dark Universe* **5-6** (2014) 18 [arXiv:1308.4955] [INSPIRE].

[80] M. Backović, A. Martini, O. Mattelaer, K. Kong and G. Mohlabeng, *Direct Detection of Dark Matter with MadDM v.2.0*, *Phys. Dark Univ.* **9-10** (2015) 37 [arXiv:1505.04190] [INSPIRE].

[81] F. Ambrogi et al., *MadDM v.3.0: a Comprehensive Tool for Dark Matter Studies*, *Phys. Dark Univ.* **24** (2019) 100249 [arXiv:1804.00044] [INSPIRE].

[82] S. Cassel, *Sommerfeld factor for arbitrary partial wave processes*, *J. Phys. G* **37** (2010) 105009 [arXiv:0903.5307] [INSPIRE].

[83] T.R. Slatyer, *The Sommerfeld enhancement for dark matter with an excited state*, *JCAP* **02** (2010) 028 [arXiv:0910.5713] [INSPIRE].

[84] S. Mizuta and M. Yamaguchi, *Coannihilation effects and relic abundance of Higgsino dominant LSP(s)*, *Phys. Lett. B* **298** (1993) 120 [hep-ph/9208251] [INSPIRE].

[85] M. Cirelli, A. Strumia and M. Tamburini, *Cosmology and Astrophysics of Minimal Dark Matter*, *Nucl. Phys. B* **787** (2007) 152 [arXiv:0706.4071] [INSPIRE].

[86] C. Dessert, J.W. Foster, Y. Park, B.R. Safdi and W.L. Xu, *Higgsino Dark Matter Confronts 14 years of Fermi Gamma Ray Data*, arXiv:2207.10090 [INSPIRE].

[87] D. Tucker-Smith and N. Weiner, *Inelastic dark matter*, *Phys. Rev. D* **64** (2001) 043502 [hep-ph/0101138] [INSPIRE].

[88] J. Bramante, P.J. Fox, G.D. Kribs and A. Martin, *Inelastic frontier: Discovering dark matter at high recoil energy*, *Phys. Rev. D* **94** (2016) 115026 [arXiv:1608.02662] [INSPIRE].

[89] PandaX collaboration, *A search for two-component Majorana dark matter in a simplified model using the full exposure data of PandaX-II experiment*, *Phys. Lett. B* **832** (2022) 137254 [arXiv:2205.08066] [INSPIRE].

JHEP01(2023)014

[90] D.P. Finkbeiner, T.R. Slatyer, N. Weiner and I. Yavin, *PAMELA, DAMA, INTEGRAL and Signatures of Metastable Excited WIMPs*, *JCAP* **09** (2009) 037 [arXiv:0903.1037] [INSPIRE].

[91] M. Carrillo González and N. Toro, *Cosmology and signals of light pseudo-Dirac dark matter*, *JHEP* **04** (2022) 060 [arXiv:2108.13422] [INSPIRE].

[92] N. Song, S. Nagorny and A.C. Vincent, *Pushing the frontier of WIMPy inelastic dark matter: Journey to the end of the periodic table*, *Phys. Rev. D* **104** (2021) 103032 [arXiv:2104.09517] [INSPIRE].

[93] HESS, HAWC, VERITAS, MAGIC, H.E.S.S. and FERMI-LAT collaborations, *Combined dark matter searches towards dwarf spheroidal galaxies with Fermi-LAT, HAWC, H.E.S.S., MAGIC, and VERITAS*, *PoS* **ICRC2021** (2021) 528 [arXiv:2108.13646] [INSPIRE].

[94] FERMI-LAT collaboration, *The Fermi Galactic Center GeV Excess and Implications for Dark Matter*, *Astrophys. J.* **840** (2017) 43 [arXiv:1704.03910] [INSPIRE].

[95] H.E.S.S. collaboration, *Search for Dark Matter Annihilation Signals in the H.E.S.S. Inner Galaxy Survey*, *Phys. Rev. Lett.* **129** (2022) 111101 [arXiv:2207.10471] [INSPIRE].

[96] X.-L. Chen and M. Kamionkowski, *Particle decays during the cosmic dark ages*, *Phys. Rev. D* **70** (2004) 043502 [astro-ph/0310473] [INSPIRE].

[97] N. Padmanabhan and D.P. Finkbeiner, *Detecting dark matter annihilation with CMB polarization: Signatures and experimental prospects*, *Phys. Rev. D* **72** (2005) 023508 [astro-ph/0503486] [INSPIRE].

[98] T.R. Slatyer, N. Padmanabhan and D.P. Finkbeiner, *CMB Constraints on WIMP Annihilation: Energy Absorption During the Recombination Epoch*, *Phys. Rev. D* **80** (2009) 043526 [arXiv:0906.1197] [INSPIRE].

[99] PLANCK collaboration, *Planck 2018 results. VI. Cosmological parameters*, *Astron. Astrophys.* **641** (2020) A6 [arXiv:1807.06209] [INSPIRE].

[100] J.M. Cline and P. Scott, *Dark Matter CMB Constraints and Likelihoods for Poor Particle Physicists*, *JCAP* **03** (2013) 044 [arXiv:1301.5908] [INSPIRE].

[101] T.R. Slatyer, *Indirect dark matter signatures in the cosmic dark ages. I. Generalizing the bound on s-wave dark matter annihilation from Planck results*, *Phys. Rev. D* **93** (2016) 023527 [arXiv:1506.03811] [INSPIRE].

[102] Y.F. Chan, M. Low, D.E. Morrissey and A.P. Spray, *LHC Signatures of a Minimal Supersymmetric Hidden Valley*, *JHEP* **05** (2012) 155 [arXiv:1112.2705] [INSPIRE].

[103] J. Berger, K. Jedamzik and D.G.E. Walker, *Cosmological Constraints on Decoupled Dark Photons and Dark Higgs*, *JCAP* **11** (2016) 032 [arXiv:1605.07195] [INSPIRE].

[104] E. Izaguirre, G. Krnjaic and B. Shuve, *Discovering Inelastic Thermal-Relic Dark Matter at Colliders*, *Phys. Rev. D* **93** (2016) 063523 [arXiv:1508.03050] [INSPIRE].

[105] D. Curtin et al., *Long-Lived Particles at the Energy Frontier: The MATHUSLA Physics Case*, *Rept. Prog. Phys.* **82** (2019) 116201 [arXiv:1806.07396] [INSPIRE].

[106] A. Berlin and F. Kling, *Inelastic Dark Matter at the LHC Lifetime Frontier: ATLAS, CMS, LHCb, CODEX-b, FASER, and MATHUSLA*, *Phys. Rev. D* **99** (2019) 015021 [arXiv:1810.01879] [INSPIRE].

[107] FASER collaboration, *FASER's physics reach for long-lived particles*, *Phys. Rev. D* **99** (2019) 095011 [arXiv:1811.12522] [INSPIRE].

JHEP01(2023)014

[108] J.M. Cornwall, D.N. Levin and G. Tiktopoulos, *Derivation of Gauge Invariance from High-Energy Unitarity Bounds on the s Matrix*, *Phys. Rev. D* **10** (1974) 1145 [INSPIRE].

[109] C.E. Vayonakis, *Born Helicity Amplitudes and Cross-Sections in Nonabelian Gauge Theories*, *Lett. Nuovo Cim.* **17** (1976) 383 [INSPIRE].

[110] M.S. Chanowitz and M.K. Gaillard, *The TeV Physics of Strongly Interacting W's and Z's*, *Nucl. Phys. B* **261** (1985) 379 [INSPIRE].

[111] M. Kawasaki, K. Kohri and T. Moroi, *Big-Bang nucleosynthesis and hadronic decay of long-lived massive particles*, *Phys. Rev. D* **71** (2005) 083502 [astro-ph/0408426] [INSPIRE].

[112] K. Jedamzik, *Big bang nucleosynthesis constraints on hadronically and electromagnetically decaying relic neutral particles*, *Phys. Rev. D* **74** (2006) 103509 [hep-ph/0604251] [INSPIRE].

[113] J. Hisano, T. Moroi, K. Tobe and M. Yamaguchi, *Lepton flavor violation via right-handed neutrino Yukawa couplings in supersymmetric standard model*, *Phys. Rev. D* **53** (1996) 2442 [hep-ph/9510309] [INSPIRE].

[114] L. Calibbi and G. Signorelli, *Charged Lepton Flavour Violation: An Experimental and Theoretical Introduction*, *Riv. Nuovo Cim.* **41** (2018) 71 [arXiv:1709.00294] [INSPIRE].

[115] L. Calibbi, R. Ziegler and J. Zupan, *Minimal models for dark matter and the muon g−2 anomaly*, *JHEP* **07** (2018) 046 [arXiv:1804.00009] [INSPIRE].

[116] A. Crivellin, F. Kirk, C.A. Manzari and M. Montull, *Global Electroweak Fit and Vector-Like Leptons in Light of the Cabibbo Angle Anomaly*, *JHEP* **12** (2020) 166 [arXiv:2008.01113] [INSPIRE].

[117] T. Toma and A. Vicente, *Lepton Flavor Violation in the Scotogenic Model*, *JHEP* **01** (2014) 160 [arXiv:1312.2840] [INSPIRE].

[118] MUON G-2 collaboration, *Final Report of the Muon E821 Anomalous Magnetic Moment Measurement at BNL*, *Phys. Rev. D* **73** (2006) 072003 [hep-ex/0602035] [INSPIRE].

[119] MUON G-2 collaboration, *Measurement of the Positive Muon Anomalous Magnetic Moment to 0.46 ppm*, *Phys. Rev. Lett.* **126** (2021) 141801 [arXiv:2104.03281] [INSPIRE].

[120] MEG collaboration, *Search for the lepton flavour violating decay $\mu^+ \to e^+\gamma$ with the full dataset of the MEG experiment*, *Eur. Phys. J. C* **76** (2016) 434 [arXiv:1605.05081] [INSPIRE].

[121] M.J. Strassler and K.M. Zurek, *Echoes of a hidden valley at hadron colliders*, *Phys. Lett. B* **651** (2007) 374 [hep-ph/0604261] [INSPIRE].

[122] M.J. Strassler, *Possible effects of a hidden valley on supersymmetric phenomenology*, hep-ph/0607160 [INSPIRE].

[123] T. Han, Z. Si, K.M. Zurek and M.J. Strassler, *Phenomenology of hidden valleys at hadron colliders*, *JHEP* **07** (2008) 008 [arXiv:0712.2041] [INSPIRE].

[124] M. Baumgart, C. Cheung, J.T. Ruderman, L.-T. Wang and I. Yavin, *Non-Abelian Dark Sectors and Their Collider Signatures*, *JHEP* **04** (2009) 014 [arXiv:0901.0283] [INSPIRE].

[125] C. Cheung, J.T. Ruderman, L.-T. Wang and I. Yavin, *Lepton Jets in (Supersymmetric) Electroweak Processes*, *JHEP* **04** (2010) 116 [arXiv:0909.0290] [INSPIRE].

[126] A. Falkowski, J.T. Ruderman, T. Volansky and J. Zupan, *Hidden Higgs Decaying to Lepton Jets*, *JHEP* **05** (2010) 077 [arXiv:1002.2952] [INSPIRE].

JHEP01(2023)014

[127] A. Falkowski, J.T. Ruderman, T. Volansky and J. Zupan, *Discovering Higgs Decays to Lepton Jets at Hadron Colliders*, *Phys. Rev. Lett.* **105** (2010) 241801 [arXiv:1007.3496] [INSPIRE].

[128] CMS collaboration, *Search for long-lived particles decaying to a pair of muons in proton-proton collisions at* $\sqrt{s} = 13$ *TeV*, arXiv:2205.08582 [INSPIRE].

[129] ATLAS collaboration, *Search for light long-lived neutral particles that decay to collimated pairs of leptons or light hadrons in pp collisions at* $\sqrt{s} = 13$ *TeV with the ATLAS detector*, arXiv:2206.12181 [INSPIRE].

[130] CMS collaboration, *Inclusive nonresonant multilepton probes of new phenomena at* $\sqrt{s} = 13$ *TeV*, *Phys. Rev. D* **105** (2022) 112007 [arXiv:2202.08676] [INSPIRE].

[131] ATLAS collaboration, *Search for Third-Generation Vectorlike Leptons in pp Collisions at* $\sqrt{s} = 13$ *TeV with the ATLAS detector*, ATLAS-CONF-2022-044.

[132] G.D. Kribs, G. Lee and A. Martin, *Effective field theory of Stückelberg vector bosons*, *Phys. Rev. D* **106** (2022) 055020 [arXiv:2204.01755] [INSPIRE].

[133] J. Aebischer, W. Altmannshofer, E.E. Jenkins and A.V. Manohar, *Dark matter effective field theory and an application to vector dark matter*, *JHEP* **06** (2022) 086 [arXiv:2202.06968] [INSPIRE].

JHEP01(2023)014